TÉCNICO LISBOA

Flexible organic light-emitting diodes

Thaís Marques Choti Pereira

Thesis to obtain the Master of science Degree in

Bioengineering and Nanosystems

Supervisor: Prof. Jorge Manuel Ferreira Morgado

Examination Committee

Chairperson: Prof. Gabriel António Amaro Monteiro
Supervisor: Prof. Jorge Manuel Ferreira Morgado
Members of the Committee: Doutora Ana Maria de Matos Charas

July 2021

“The task is not so much to see what no one has yet seen; but to think what nobody has yet thought, about that which everybody sees.”

Arthur Schopenhauer

Preface

The work presented in this thesis was performed at Instituto de Telecomunicações of Instituto Superior Técnico (Lisbon, Portugal), during the period October 2020-July 2021, under the supervision of Prof. Jorge Morgado.

Acknowledgment

So much to be thankful for,

But first I would like to thank God for always being present and giving me strength throughout the process.

To my parents, Wilson and Deise Pereira for being my greatest support and example not only in the final stage but throughout my entire trajectory.

To my supervisor, Professor Jorge Morgado for all the support and effort provided during this work, as he was present not only during the practical work, but also all the effort to be present throughout the process.

To my love, Ricardo, throughout the writing process you were supporting me even when I thought I wouldn't make it.

To everyone who was present, directly, or indirectly involved in the writing process, giving me their support, and understanding, my eternal thanks.

I declare that this document is na original work of my own authorship and that it fulfils all the requirements of the Code of Conduct and Good Practices of the Universidade de Lisboa

Abstract

Since the first report of electroluminescence observation in organic materials, both small molecules and polymers, the field of organic light-emitting diodes (OLEDs) has greatly expanded, covering various application areas such as displays and lighting. In view of the unique mechanical properties of the organic materials, flexible OLEDs are being developed for integration in buildings and furniture and for biomedical applications, namely sensors. OLEDs are key components of the Internet of Things paradigm. In this project, different materials were studied for the manufacture of OLEDs, to obtain the best performing ones in terms of luminance and efficiency, providing benchmarking systems to be replicated in flexible OLEDs. Within this project we achieved flexible OLEDs, fabricated on PET/ITO substrates, with a luminance of 663 cd/m^2, 0.45 cd/A luminance efficiency and 0.36% external quantum efficiency.

KEYWORDS: Light-emitting diodes (OLEDs), flexible OLEDs, electroluminescence, organic materials

Resumo

Desde o primeiro relato de observação da eletroluminescência em materiais orgânicos, sejam pequenas moléculas ou polímeros, o campo dos diodos emissores de luz orgânicos (OLEDs) expandiu bastante, de forma a abranger várias áreas de aplicação, como monitores e iluminação. Em vista das propriedades mecânicas exclusivas dos materiais orgânicos, OLEDs flexíveis estão sendo desenvolvidos para integração em edifícios e em móveis e para aplicações biomédicas, nomeadamente sensores. OLEDs são componentes-chave do paradigma da Internet das Coisas. Neste projeto, foram estudados diferentes materiais para o fabrico de OLEDs, visando otimizar a sua performance, em termos de luminância e eficiência, para servirem de referência e seremreplicados em dispositivos OLEDs flexíveis. OLEDs flexíveis, fabricados em substratos de PET/ITO com luminância de 663 cd/m^2, eficiência de luminância de 0,45 cd/A e eficiência quânticaexterna de 0,36%.

PALAVRAS-CHAVE: Díodos emissores de luz (OLEDs), OLEDs flexíveis, eletroluminescência, materiais orgânicos

Index

List of Figures

List of Tables

Objectives

This project aims to develop flexible organic light-emitting diodes (OLEDs). To achieve this goal, the sequential sub-objectives were proposed:

a) Fabrication and characterization of OLEDs on ITO-coated glass substrates.

b) Assessment of the characteristics of OLEDs based on polymer blends and blends combining polymers and a phosphorescent complex.

c) Optimization of PEDOT: PSS to replace ITO as electrode.

d) Fabrication and characterization of flexible OLEDs on PET/ITO substrates.

1 Introduction

This chapter addresses the relevance of the light-emitting diodes (LEDs) for our daily lives and their scientific and technological (S&T) evolution.

The first devices were based on inorganic semiconductors but, more recently, LEDs based on organic semiconductors, OLEDs, have become the center of a new S&T revolution, by the simplicity of fabrication and their mechanical properties, namely their flexibility. The project is focused on organic light-emitting diodes.

In search of a new field of research aimed at the foundation and deepening themes pertinent to the aspirations of society, the development of flexible organic light-emitting diodes emerges as a pillar where some relevant research is inserted. The field of organic materials has greatly expanded, and OLEDs are a key for Internet of Things paradigm which consist on the combination of advanced data analytic capabilities and everyday objects, transforming how we work and live.

1.1Societal relevance of light-emitting diodes

There are two main areas where LEDs became key players: lighting and displays, aside their application in a variety of devices such as sensors and photodetectors. And there has also been interest in adapting OLED technology for applications beyond the display and lighting sector, e.g., for biomedical use or optical communications.
Organic light emitting diodes (OLEDs) are a promising energy alternative for the future and are therefore one of the most interesting organic devices.

1.1.1 Lighting

Lighting directly influences the performance of visual tasks, making critical task details visible. The evolution of lighting sources has evolved from flames (fires and candles) to electrical lamps of various types (namely incandescent and fluorescent tubes). However, the efficiency of these light sources is limited by a significant emission in the infrared spectral range (away from the visible 400-700nm), meaning that energy is lost as heat.

Light-emitting diodes offer the possibility to strongly reduce (or even suppress) that energy dissipation mechanism, leading to higher efficiencies (and concomitant energy saving) and the ability to optimize the quality of light. This solid-state lighting can use LEDs based on inorganic semiconductors and organic light-emitting diodes organic (OLED), based on small molecules or electroluminescent polymers (PLED), to replace the traditional electrical filaments, plasma (used in arc lamps, such as fluorescent lamps) or gas.

1.1.2 Displays

Images on screens are created by pixels. The old TV screens were based on a phosphorescent screen and an electron beam that would scan the entire screen, line by line, defining dark and light spots that made an image. Today, each pixel is addressed individually, as is the case of the well-known Liquid Crystals Displays (LCD), where a pixel would act as a switch (ON/OFF) for light transmittance from a backlight source. A full-color screen requires three main colors (red, green, and blue, RGB). Therefore, to define an image point, we need the three colors, whose relative intensity allows the “creation” of a full spectrum of colors. Displays based on (O)LEDs use three of such devices, emitting in the red, green, and blue, to define an image point. This implies that each (O)LED must be addressed individually, which is done by associating a driving circuit (containing transistors and capacitors) to each (O)LED. There are currently two different approaches to create images on displays, passive, and active matrix.

1.1.2.1 PMOLED – Passive Matrix OLED

A PMOLED display uses a simple control scheme in which each row and line on the display is controlled sequentially (one at a time). PMOLED electronics do not contain a storage capacitor and therefore each line contains pixels which are off most of the time. To compensate, you would

need to use more voltage to make them brighter. In the passive matrix, OLEDs are positioned at the intersections of the addressed pairs of anodes and cathodes, being the anode strips arranged perpendicular to the cathode strips. The intersections of the cathode and anode make up the pixels where light is emitted. External circuity applies current to selected strips of anode and cathode, determining which pixels get turned on and which pixels remain off (Kijima *et al*, 1997) and has been commercialized since 1999. (Chang *et al*, 2001)

Therefore, although PMOLEDs are easy and cheap to manufacture, they are not efficient and OLED materials have a shorter service life (due to the high voltage required). PMOLED displays are also restricted in resolution and size because the more lines you have, the more voltage you need to use.

1.1.2.2 AMOLED – Active Matrix OLED

AMOLEDs have complete layers of cathode, organic molecules and anode, but the anode layer overlaps a set of at least two thin-film transistors (TFT) (the first to start and stop charging a storage capacitor and the second to provide a voltage necessary to create a constant current for the pixel). The TFT array itself is the circuit that determines which pixels are activated to form an image. AMOLEDs consume less power than PMOLEDs because the TFT array requires less power than an external circuit. (Stewart et al, 2001).

Since 2007, AMOLED technology has been used in mobile phones, media players, TVs and digital cameras, and it has continued to make progress toward low-power, low-cost, high resolution and large size applications. (Lee *et al*, 2010) AMOLED displays provide higher refresh rates than passive-matrix, often reducing the response time to less than a millisecond, and they consume significantly less power. This advantage makes active-matrix OLEDs well-suited for portable electronics, where power consumption is critical to battery lifetime. (Suyko, 2009)

1.1.2.3 Differences between PMOLED and AMOLED

- Active matrix controls the pixel individually, passive do not.
- AMOLED contains a storage capacitor, PMOLED do not.

The main advantage of AMOLED over PMOLED is its size. The TFT backplane is responsible for maintaining active pixel states and controlling the pixels individually allowing OLED displays to be physically larger and of high resolution. PMOLED displays are generally smaller in size and resolution due to the inherent disadvantage of the scheme passive array addressing but it is worth mentioning that a critical advantage of PMOLED over AMOLED is that it is easier to fabricate and cheaper to manufacture.

The differences do not make one better than other, just make them useful for different purposes.

1.2 Organic light-emitting diodes structure and processes

OLED technology has received great attention from industry and academia over the past three decades due to its obvious advantages such as easy preparation, low cost, safe application, light weight, low driving voltage and quick response. (Reineke *et all*, 2013). Organic light-emitting diodes (OLEDs) have drawn enormous attention due to their outstanding performance in high-quality full-color display and solid-state lighting applications.

An OLED typically consists of a stack of organic layers between an anode and a cathode, at least one of which is partially transparent. In organic EL devices, the generation of light is the consequence of recombination of injected holes and electrons of the electrodes. In a chemical sense, the reaction of radical cations (holes) and radical anions (electrons) provide excited molecules that emit light as one of the decay processes. (Kido *et al*, 1995)

Many studies were made and discovered that it is possible to produce OLEDs from different ways. This is discussed in the next topics.

1.2.1 Single layer devices

The final purpose of an OLED structure is to create an excited state (exciton) in a molecule (being it of low molecular weight or polymer). By similarity between the emission spectra resulting from photon excitation (fluorescence or photoluminescence) or from electrical excitation, it was concluded that the same emissive excited state was formed. The scheme below compares, in a very simple way, the two processes (photoexcitation and electrical excitation).

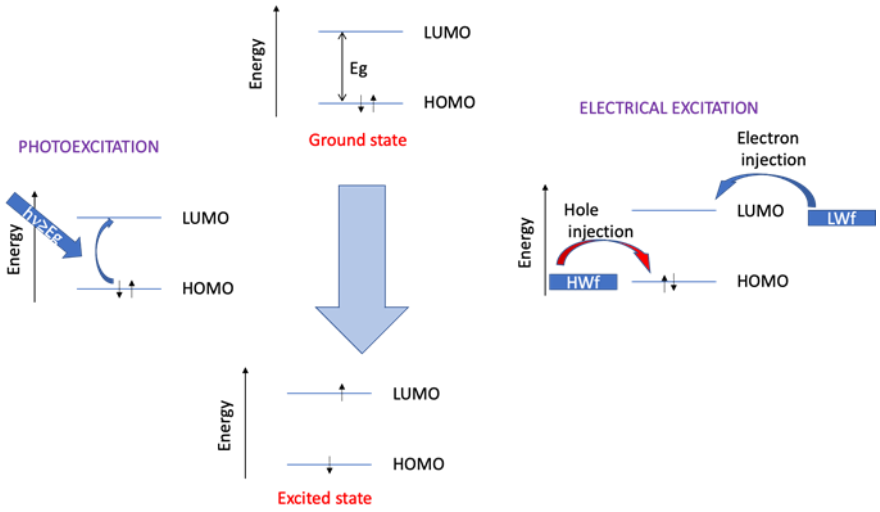

Scheme 1. Comparison between Photoexcitation and Electrical Excitation (HWf: high work function electrode; LWf: low work function electrode).

The basic structure of an OLED would be a sandwich-like structure. The electroluminescent film is sandwiched between two electrodes with different work functions and appropriate to, upon a voltage application, inject electrons in the LUMO and inject holes in (or remove electrons from) the HOMO of the electroluminescent molecule/polymer. One of the electrodes needs to be transparent to allow the escaping of the generated light. This would be a single-layer OLED. Typically, we use a mixed indium-tin oxide (ITO) deposited on glass (to inject holes) and, as the low work function electrode, a metal such as aluminum or calcium (which is usually coated with a protecting layer of aluminum).

Sometimes, ITO is coated with a hole-injecting layer made of a conductive polymer blend: poly (3,4-ethylenedioxythiophen) doped with polystyrene sulfonic acid (PEDOT: PSS). It has the dual role of planarizing the ITO surface and to increase ITO work function (from ca. 4.8 to 5.1 eV), thereby improving the hole injection ability. Such devices are represented as ITO/PEDOT: PSS/Emissive layer/Ca/Al.

In general, only singlet excited states can decay radiatively. Therefore, to maximize the emission efficiency, it is important that a balance of holes and electrons population is reached in the bulk of the emissive layer (maximizing the exciton formation per injected electron). This balance depends not only on the injection barriers (energy mismatch between PEDOT: PSS work function and the HOMO and between the Ca work function and the LUMO) but also on the relative mobilities of the two charge carriers within the emissive layer.

The spins of the injected charges (holes and electrons) are unrelated. This means that the excited state may have either a total spin of zero or one, that is, the electrically formed excitons may be either singlets or triplets, respectively. In statistical terms, 25% of the formed excitons are singlets and 75% are triplets, as the multiplicity of the singlets is one (2S+1=1) and that of the triplets is three (2S+1=3). This contrasts with the excitons formed upon photon absorption that are all singlets. In general, only the singlets decay radiatively.

The structure of OLEDs was initiated with a single layer (described above) and gradually evolved to double layer and triple layer and to their current multilayer arrangement. Even though multilayer organic light-emitting devices (OLEDs) are known to be more efficient than single-layer OLEDs,

single-layer OLEDs remain very interesting, in particular for materials characterization, due to their simple structure. (Kim *et al*, 2005).

This single layer OLEDs are less efficient because the injection and transport of both holes and electrons should occur in a balanced way, which is difficult to maintain, so to obtain higher efficiency, OLEDs made with multilayers were studied, some of which are explained below.

1.2.2 Materials

Organic emitters play a vital role in determining the overall performance of organic light-emitting diode (OLED) devices. According to their emitters, OLEDs can be classified into different groups.

1.2.2.1. SMOLED – Small Molecule OLED

According to Duan *et al* (2010) small molecules have advantages such as easy synthesis and purification. Usually, the production of small molecule devices and displays involves the process of thermal evaporation under vacuum, making their production more expensive and of limited use for large area devices. However, unlike polymer-based devices, the vacuum deposition process allows for the formation of well-controlled homogeneous films and the construction of very complex multilayer structures. Due to this high flexibility in the layer design, the formation of distinct charge transport and blocking layers is possible, being the main reason for the high efficiency of small molecule OLEDs.

1.2.2.2. PLED – Polymer LED

A polymer LED is a type of OLED that uses polymers as the electroluminescent semiconducting material to produce very thin LEDs that can be used for many applications. The low processing cost and possibility of large area displays endowed PLEDs with the potential of being a disruptive technology that is attractive for industrial applications in display and lighting. (Minshal *et al*, 2007) The technology also offers a great deal of promise as a basis for cheaper, simpler lighting sources.

Chen *et al* (2010) affirms that the PLED typical device architecture might be a hybrid structure consisting of polymer and layers sandwiched between two metal electrodes or pure organic structure where all emissive and carrier layer are organic materials.

The main problem that prevents the commercial use of PLEDs is that the lifetimes are often still very short, usually caused by defects due to synthetic by-products or degradation of the emissive polymers, usually by oxidation. (Grimsdale *et al*, 2009)

1.2.3 Multilayer OLEDs

Udhiarto *et al* (2016) explain that multilayer structures, incorporating hole transport layer, electron transport layer and/or hole injection layer, can effectively exhibit reduced turn-on operating voltage as well as increased luminance.

A multilayer device consists of an emission layer (EL) sandwiched between the hole and the electron transport layers (HTL and ETL, respectively). This general structure serves three main purposes:

I. Facilitates the injection of charge carriers by reducing the respective injection barriers.

II. The recombination of electrons and holes in the emissive layer is increased due to accumulation of charges in the EL (load carriers are blocked by opposite transport layer - the HTL is a barrier to electrons and ETL to the holes)

III. The recombination zone is shifted towards the device and thus the extinction of excitons by the electrodes is avoided. (Nuyken *et al*, 2006)

A multilayer OLED structure can be observed in the next figure.

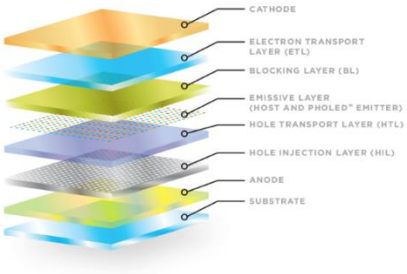

Figure 1.1 Structure of a multilayer OLED - https://oled.com/oleds/ on June 14th.

The first layer in OLEDs structures is the substrate which will support the OLED. It can be made from different materials, such as glass or a flexible material, as PET.

The main component in an OLED display is the emitter - an organic (carbon-based) material that emits light when electricity is applied. The basic structure of an OLED is an emissive layer between a cathode (which injects electrons) and an anode (which removes electrons – holes). In an OLED a high charge carrier mobility is not crucial as what is required is balanced charge carrier mobilities, i.e., the holes and electrons should have similar mobilities to promote recombination within the emissive layer.

Under a direct bias (positive potential applied to the anode (e.g., ITO) and negative potential applied to the cathode (e.g aluminum)), as the electricity starts to flow, holes are injected from the anode (positive terminal) and electrons from the cathode (negative terminal). Charge carriers move through transport layers and they meet in the emission layer, where excitons (excited neutral states or electron-hole pairs) are formed.

The hole injection layer (HIL) should facilitate injection from the anode to the hole transport layer (HTL). This can be achieved by selecting the material with the appropriate energy of the highest occupied molecular orbital (HOMO) so that it is between the HOMO of the HTL and the ionization potential of the anode..

The hole transport layer must have high mobility of the holes and must prevent the electrons coming from the cathode from reaching the anode (giving rise to a shunt current). Furthermore, the optical transmission of all organic layers must be high in the region of the emission wavelength. Organic EMLs play a dominant role in deciding the performance of OLED device such as color and efficiency. (Sliney, 2007)

Blocking layer (BL): commonly used to improve OLED technology by confining electrons (charge carriers) to the emissive layer. It may also be used between the HTL and the EML to confine holes.

The properties of the electron transport (ETL) and electron injection (EIL) layers is complementary to those already described for the HIL and HTL layers. The anode must have a high ionization potential to inject holes into the HOMO of the HIL. Therefore, the cathode must be a metal with a low working function, such as magnesium or calcium. Finally, at least one electrode must be transparent to achieve high light extraction efficiency. For this reason, ITO (Indium-Tin Oxide) is used as the transparent anode in most cases. (Posada *et all*, 2008)

According to Karzazi (2013), the efficiency of the OLED, that is, the electron-to-photon conversion capacity, can be directly evaluated by the quantum efficiency (QE). QE refers to the numerical ratio of photons to the injected electron-hole pairs, which still represents a great challenge for OLED devices until today. Charge injection plays an important role (along with transport) due to the strong influence on the electron/hole balance in the device and therefore on the exciton population.

1.3 Fabrication and characterization of OLEDs

1.3.1 Electrodes and active layer deposition

The deposition process of the layers was done through the spin coating process, which consists on the application of a small amount of coating material (the conjugated polymers) to the center of the substrate (glass or PET), the substrate is then rotated at a speed of up to 10,000 rpm to spread the coating material by centrifugal force to make it uniform. Rotation is continued while the fluid spins off the edges of the substrate (Cohen and Lightfoot, 2011). The concentration of the solution and spinning speed directly influence the thickness of the deposited layer.

The electrodes deposition was carried out in a nitrogen-filled glove box to preventtheir oxidation by atmospheric oxygen and/or water. Using the thermal evaporation method, the material to be deposited is transformed into a gaseous state when heated. Tungsten filaments are used to generate heat by the Joule effect. Organic and inorganic materials are placed inside ceramic crucibles which are heated by the tungsten filament. Once the evaporation or sublimation temperatures are reached, the particles are ejected and deposited on top of the desired layer. Particle momentum is crucial for defining a good layer. If the particles have a very high momentum, they can degrade the layer where they are being deposited. (Reichelt and Jiang, 1990).

1.3.2 OLEDs characteristics

To compare different materials and device architectures, reliable and accurate measurements of device efficiency are crucial (Anaya *et al*, 2019), this is some OLEDs characteristics to be aware during the process of production.

- Current Voltage Luminance

The current-voltage-luminance (IVL) measurement is the basic characterization method for OLEDs.

The current-voltage curve is measured as in the normal IV (relationship between the electric current through a circuit, device, or material, and the corresponding voltage, or potential difference across it.). Additionally, the steady-state emission of the OLED is recorded using a photodetector. Knowing the spectrum of the OLED and the sensitivity and geometry of the photodetector the electrical and optical efficiency of the OLED can be calculated.

- Luminance Calculations

Luminance is the intensity of light coming from a particular planar source. It is interpreted as the ratio of light intensity in that direction, produced by an element of surface surrounding the point, to the area of the orthogonal projection of the surface element on a plane perpendicular to the given direction. To measure the light intensity one must first take a reference direction for measurements, and then determine the solid angle used therein. For applications in displays, the reference direction should be chosen as the perpendicular to the surface of the OLED (supposed line of sight). (Posada *et al*, 2008)

Assuming a Lambertian intensity profile and a source of discoidal aspect with radius r, the light intensity on a point detector placed at a distance d can be expressed as follows:

$$I = I_0 \left({r^2}/{(r^2 + d^2)} \right) \quad (1.1)$$

For a detector with a finite area, this expression can be used provided that the detector exhibits a sufficiently small solid angle. The recommended condition by is that Ω <0.01sr. Under these conditions, the luminous intensity (Λ, in candela) can be obtained by comparing the PLED signal with that obtained with a calibrated lamp. The luminance is then given as:

$$L = {\Lambda}/{\pi r^2} \quad (1.2)$$

- Efficiency Calculations

The current efficiency can be calculated as the amount of current flowing through the device, J, with an emissive area, S, required to produce a certain luminance, L, expressed by equation 1.3 cd / A

$$EL\ eff = \frac{L}{J} = \frac{LS}{I} \quad (1.3)$$

The luminous power efficiency is a quantity of measurement for light sources and is described as the ratio of luminous flux to power. Essentially, it tells us how much light is being given compared to the amount of electricity used. This efficiency is measured in lm/W.

The External Quantum Efficiency, E.Q.E., is given by the ratio between the number of photons emitted from the surface of the device and the number of injected electrons. (De Sá Pereira *et al*, 2017)

- Color Coordinates

The color of a light source is typically characterized by its CIE (*Commission Internationale de l'éclairage"*, known in English as the International Commission on Illumination) coordinates, which describe how the human eyes perceive the color emitted by a light source with two numbers, say (x, y), in the CIE chromaticity diagram (Srivastava and Ronda, 2003).

Based on the basic principles of colorimetry, several other linear combinations of RGB stimulus values can be derived that can provide better properties than the original values. The CIE 1931 color spaces are the first defined quantitative links between wavelength distributions in the visible electromagnetic spectrum and physiologically perceived colors by the human vision. The system was designed in 1931 by the "*Commission Internationale de l'éclairage*".

The commission decided to mathematically transform the data in such a way that the red, green, and blue real light sources used in the laboratory measurements were replaced by three theoretical light sources. In this system, then, any test light is characterized by three numbers ("tristimulus values"), X, Y, and Z, which are the amounts of each of the three primaries needed by the standard observer to match the test light. Y, for example, was defined to be mathematically identical to the luminance of the test light. For convenience in plotting colors graphically, the chromatic variables are characterized by the "chromaticity coordinates" which are derived from X, Y, and Z by normalizing each to their sum. (NASA Ames Research Center, found in https://colorusage.arc.nasa.gov/lum_and_chrom.php on August 8th)

The chromaticity values can also be defined in XYZ system as follows:

$$x = \frac{X}{X+Y+Z}$$

$$y = \frac{Y}{X+Y+Z} \quad (1.4)$$

$$z = \frac{Z}{X+Y+Z}$$

Large x values correspond to red or orange hues, y values correspond to green, blue-green, or yellow-green, and large z correspond to large blue, violet, or purple hues. Because x + y + z = 1, only two of these values are required. (Bull, 2014).

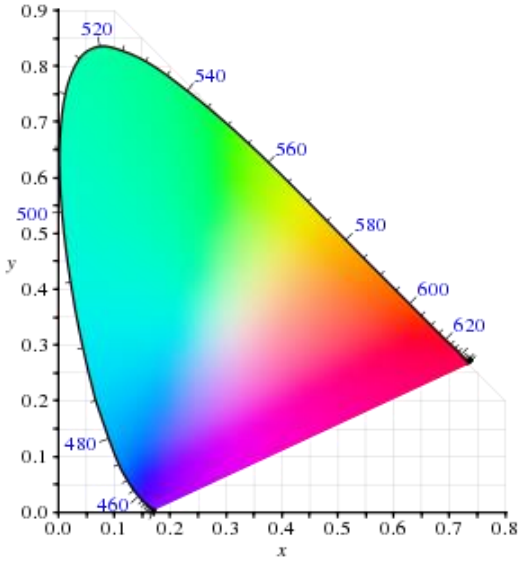

Figure1.2 Chromaticity diagram with x and y coordinates. Found in https://en.wikipedia.org/wiki/CIE_1931_color_space at July,2021

2 Experimental

For the experimental process, 12mm long square transparent substrates, made from different materials were used:

Rigid OLEDs: Glass with ITO and without ITO

Flexible OLEDs: Polyethylene terephtalate (PET) with ITO.

The first type of layers that composes the organic light emitting diode investigated in this project is a glass substrate coated with a thin layer of ITO (transparent conducting oxide).
The ITO layer used has 100 nm of thickness. ITO is a conductive material and is transparent in the visible spectral region, but almost opaque in the UV and infrared region (Gheidari *et al*, 2005), which makes this semiconductor a good option to be used as a transparent conductive oxide (TCO) (Farhan e*t al*, 2013).

Figure 2.1 shows a schematic draw of the glass/ITO and PET/ITO substrates. The ITO is etched from the sides, to avoid short circuits, leaving a central stripe, whose width (8 mm) determines the active area. A great effort is made to ensure that these dimensions are common to all substrates.

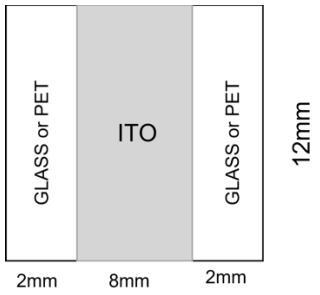

Figure 2.1 Schematic draw of glass/ITO or PET/ITO substrate

The next steps are involved in the preparation of the glass / ITO and PET/ITO substrates:

1. Adhesive tape is placed on the sides of the ITO, leaving the central part (8 mm wide) exposed.
2. It is placed some fingernail polish over the surface of substrates to protect the uncovered band.
3. The adhesive tape is removed after a couple of hours (to dry the fingernail polish).
4. Substrates are placed in a beaker with diluted aqueous hydrochloric acid at solution temperature of 100 ºC for approximately 4 min to etch the ITO on the sides. Complete ITO removal can be confirmed upon measurement of the surface resistance. Caution is taken to ensure that the fingernail polish protecting the central stripe is not destroyed.
5. After washing with plenty of tap water, the substrates are placed in a beaker with acetone in an ultrasounds bath for 5 min to remove the nail polish.
6. The glass/ITO and PET/ITO substrates are then thoroughly washed with detergent and distilled water under ultrasonic waves during 3 min. The procedure is repeated several times to ensure complete removal of remaining detergent.
7. Finally, they were washed with acetone and then isopropanol and dried under a nitrogen stream.

The glass/ITO and PET/ITO proceed for an oxygen plasma treatment (Figure 2.2). According to Sugiyama *et al* (2000), oxygen plasma treatment is a widely used process to clean the ITO (and other substrates) surfaces.This treatment is very important when PEDOT: PSS is deposited on

top (from an aqueous dispersion), as it allows a uniform film formation. The samples were placed in a chamber of a plasma machine called "PlasmaPrep$_2$" under vacuum. In the second step, the O_2 cylinder was opened, and the plasma was activated. Each treatment lasted approximately 3 min. To ensure an efficient treatment, this step was repeated once more under the same conditions, at the end of this step the vacuum was interrupted, the O_2 cylinder was closed, and the samples removed from the chamber under atmospheric pressure.

The samples then went to the deposition process using the method of spin coating. This deposition method consists of depositing a particular solution or dispersion on top of a spinning substrate during a short period of time. The concentration of the solution/dispersion and spinning speed directly influence the thickness of the deposited layer. The substrates were then coated (Figure 2.3) with a hole-injection layer of PEDOT: PSS (CLEVIOS P VP AI 4083, PEDOT:PSS ratio 1:6, from Heraeus) with a thickness of 80 nm, which was cured at 125 °C for 10min on a hot plate in air.

As emissive materials, we used some neat polymers and blends (poly(9,9-dioctylfluorene) – PFO; poly(9,9-dioctylfluorene-*alt*-benzothiadiazole) - F8BT; PFO: F8BT – F95; PFO: Ir(dmpq)$_2$(acac) - PFOIr95; poly(N-vinyl carbazole):Ir(dmpq)$_2$(acac) - PVKIr95), deposited by spin coating from toluene solution to obtain between 70 to 75 nm thick films. PFO, F8BT and the iridium complex (Ir(dmpq)$_2$(acac)) were obtained from Ossila and used as received. PVK was obtained from Aldrich.

Another study was carried out using a different PEDOT: PSS formulation (PH1000, PEDOT:PSS ratio 1:2.5 from Heraeus, supplied by Ossila) which is one of the best choices for flexible electrodes owing to its high transmittance in the visible range, high and adjustable conductivity, intrinsically high work function, excellent thermal stability, and good film-forming capability as well as superior mechanical flexibility (Hu *et al*, 2020). It is important to have a transparent highly conductive polymer that may be used in the fabrication of flexible OLEDs, replacing the ITO and avoid the necessary of using the glovebox during the fabrication.

Figure 2.2 Machine “PlasmaPrep$_2$” used for oxygen plasma treatment

Figure 2.3 Machine used for spin coating.

The device structures were completed with thermal evaporation of the calcium cathode (20–30 nm) and a protection overlayer of aluminum (100 nm) inside of a glovebox under vacuum (base pressure of ca. 10^{-6} mbar). The deposition of the Ca/Al cathode is made through a shadow mask that defines four LEDs per substrate, each with an active area of $4mm^2$. Inverted LEDs were prepared on glass substrates, coated with PEDOT: PSS+DMSO, followed by the thermal deposition of a thin layer of ZnO prepared from a precursor solution of zinc acetate, and the deposition of the active layer. The anode (on top) consists of a layer of thermally deposited molybdenum oxide (ca. 20 nm thick) coated with ca. 80 nm of aluminium. The OLEDs were measured in a home-made set up consisting on a power supply (1), a dark chamber (2), a support with 5 contacts (3) for the OLED analysis in the dark chamber, and a spectrometer Scansci connected to the computer and to the dark chamber (4) (Figure 2.4a and 2.4b) to obtain the spectra data.

a) 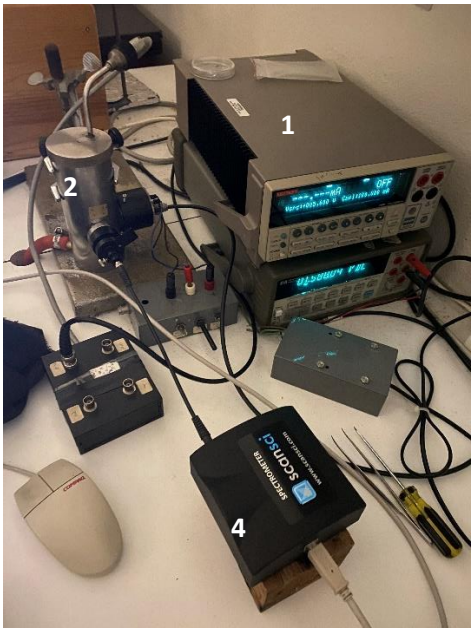

b) 

Figure 2.4 a) Complete home-made set up and b) Support with contacts for the OLED for dark analysis

The thickness of the films was measured with a profilometer (DEKTAK 6M Stylus Profiler), and the absorption was measured with a CECIL spectrophotometer. The photoluminescence spectra were obtained for films deposited on quartz substrates using illumination and emission detection.

The conductivity of polymer films deposited by spin coating on glass substrates (as used during the manufacture of OLEDs) was determined by the 4-point probe technique with a Keithley 2400 Source Meter unit and a multimeter (Agilent 34401A 6½ Digital Multimeter). For the measurements, the films were coated with a 40 nm thick Au layer deposited under high vacuum (<10^{-4} mbar) by thermal evaporation through a shadow mask to define four gold contacts equally spaced. At least 4 measurements were done in each film. (Figure 2.5a and 2.5b). Figure 2.6a and 2.6b shows the setup used for the 4-contacts measurements.

a) 

b)

Figure 2.5 a) Top view of spaced 4 gold stripes deposited by thermal evaporator and b) Gold during evaporation

a)

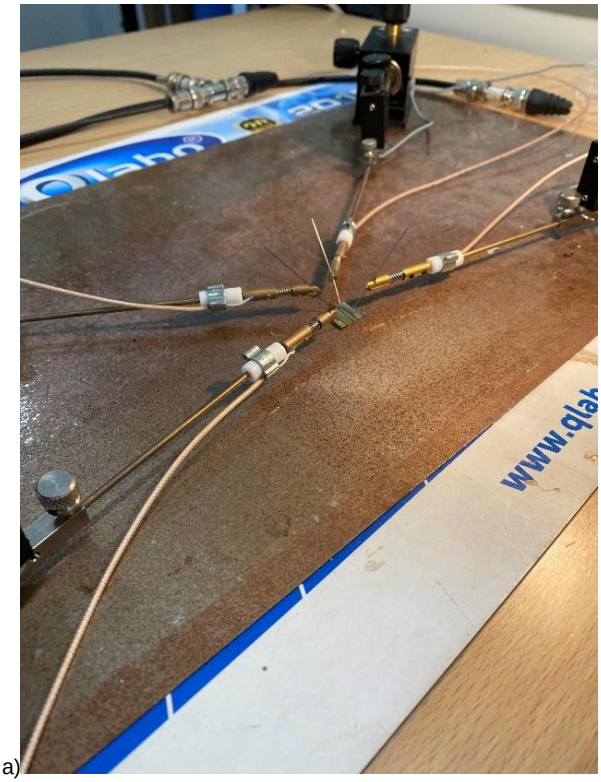

b) 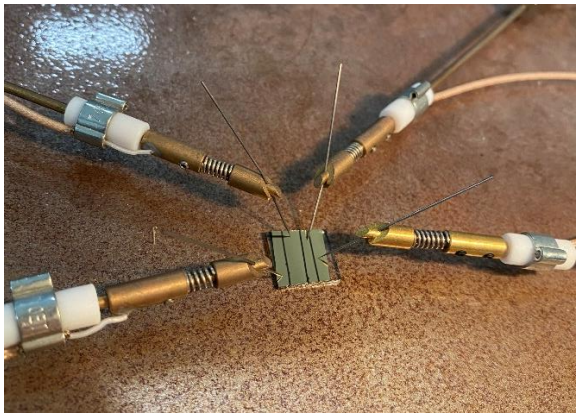

Figure 2.6 a) and b) setup used for the 4-contacts measurements

The 4-point probes technique is an electrical impedance measurement technique that uses separate pairs of current-carrying electrodes and voltage sensors. Separation of current and voltage electrodes eliminates the lead and contact resistance from the measurement. This is an advantage for precise measurement of low resistance values.

The four-point probe consists of four electrodes arranged in an equidistant linear array. In the standard configuration, a current I is fed through the sample via the two outer electrodes. This generates a voltage drop V across the two inner electrodes, which is measured by a high impedance voltmeter to determine the sample resistance. (Hansen *et al*, 2003)

During the analysis of the 4-point probes method, graphs were obtained with the difference of potential and current, where the slope of this graph will be the resistance, applying the second ohm's law:

$$R = \rho \frac{l}{S} \quad (1.5)$$

Where: R is resistance (Ω), ρ is resistivity (Ω.m), l is length (m) and S is the cross area (thickness multiplied by width) $(m^2)´$.

The resistivity and conductivity are related as shown in equation 1.6.

$$\sigma = \frac{1}{\rho} \ (1.6)$$

Where: σ is conductivity ($\Omega^{-1}.m^{-1}$) and ρ is resistivity (Ω.m).

3 Results and Discussion

We have studied first OLEDs based on single emissive materials followed by the investigation of OLEDs based on blends. The use of blends has, in general, the aim of balancing the charge transport mobility (of electrons vs holes), confine the emissive states (excitons) in isolated chains to avoid charge and exciton concentration quenching effects and/or tuning the emission colour. The study also involved the application of electrode materials that would be more adequate for the fabrication of flexible OLEDs. Along the presentation of the results, the optical (absorption and emission) properties of the materials are also presented and discussed in connection with the properties of the OLEDs incorporating them.

Here, we present the results of representative devices. A complete set of results can be found in the Appendix.

3.1. LEDs based on neat polymers

Two well-known electroluminescent conjugated polymers, poly(9,9-dioctylfluorene) and poly(9,9-dioctylfluorene-*alt*-benzothiadiazole), were initially studied to gain insight on the OLEDs fabrication and characterization. They were later used in the fabrication of OLEDs based on blends.

3.1.1 Poly(9,9-dioctylfluorene), PFO

Figure 3.1 shows the performance of a PFO-based OLED with the structure ITO/PEDOT: PSS/PFO/Ca/Al.

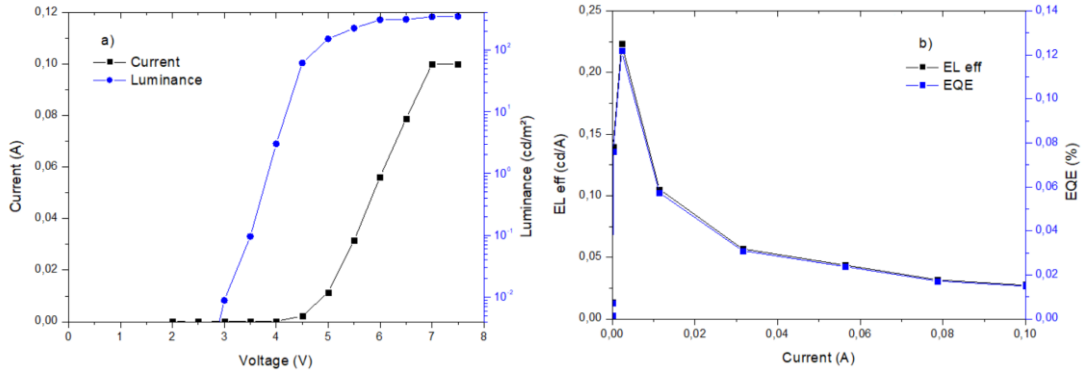

c)

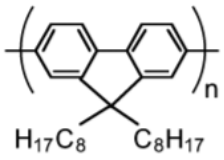

Figure 3.1. a) Current and luminance as a function of the applied voltage for an ITO/PEDOT: PSS/PFO/Ca/Al OLED, b) corresponding electroluminescence efficiency and EQE as a function of the current and c) PFO´s structure.

The device shows a light-onset voltage (voltage at which a luminance of 10^{-2} cd/m^2 is detected), of 3.2V and reaches a maximum luminance of 347.86 cd/m^2 at 7V. At this voltage, the device reaches the current limiting value (100mA) of the voltage source. The efficiency of the device shows a peak value at low current (up to ca. 0.22 cd/A and ca. 0.12%), which decreases upon increase of the driving voltage. It is possible that at higher current values there is a charge-induced quenching of the excitons.

In the calculation of the LEDs luminance a conversion factor of 1349 cd/m^2/V was used, based on the electroluminescence spectrum obtained at a driving voltage of 5.5V.

Figure 3.2 shows the electroluminescence (EL) spectra recorded for PFO-based LEDs. For comparison, the absorption, and the photoluminescence spectra of PFO films are also shown.

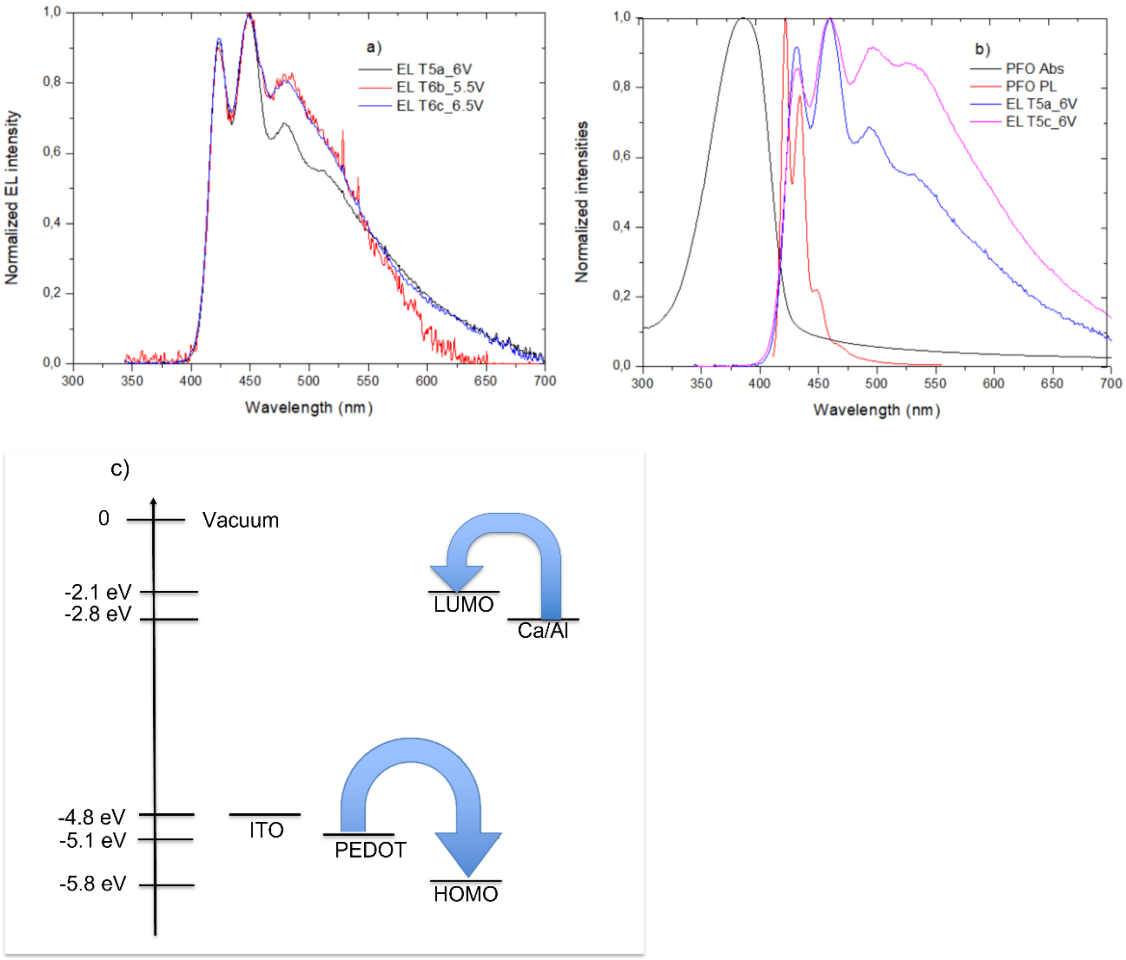

Figure 3.2. a) Normalized EL spectra of two PFO-based LEDs and b) aging effect on the EL spectrum and comparison with the absorption and photoluminescence (PL) spectra of PFO films and c) shows the energy levels diagram for the ITO/PEDOT: PSS/PFO/Ca/Al LED. The energy values are from Bernardo *et al* (2010).

PFO is a blue emitting polymer. The absorption spectrum has a maximum at ca. 380 nm and the emission spectrum usually exhibits a vibronic structure, with the first vibronic occurring at 420nm, it is possible to see that in photoluminescence of PFO the emission starts on 400 and remains until 625 nm, this variation can be seen on electroluminescence which proves that the excitation state is responsible for the emission in both cases.(As shown in Figure 3.2 b), the EL spectrum is modified at higher driving voltages, with an increased emission intensity centred at about 550 nm. This has been attributed to aggregation of PFO and/or its degradation (fluorenone moieties have been proposed to be responsible for this emission) (Grisorio *et al*, 2007). This leads to a change of the emission colour from blue (as shown in the photograph of the PFO photoluminescence in figure 3.3b) to blue-green that appears as whitish. Figure 3.3a shows the colour coordinates in the chromaticity diagram (CIE) of the blue emission calculated for the spectrum EL T5a at 6V (shown in Figure 3.2a) For comparison the color coordinates of the spectrum EL_T5c_6V are also shown. This instability strongly limits the use of PFO as the active material in blue-emitting LEDs.

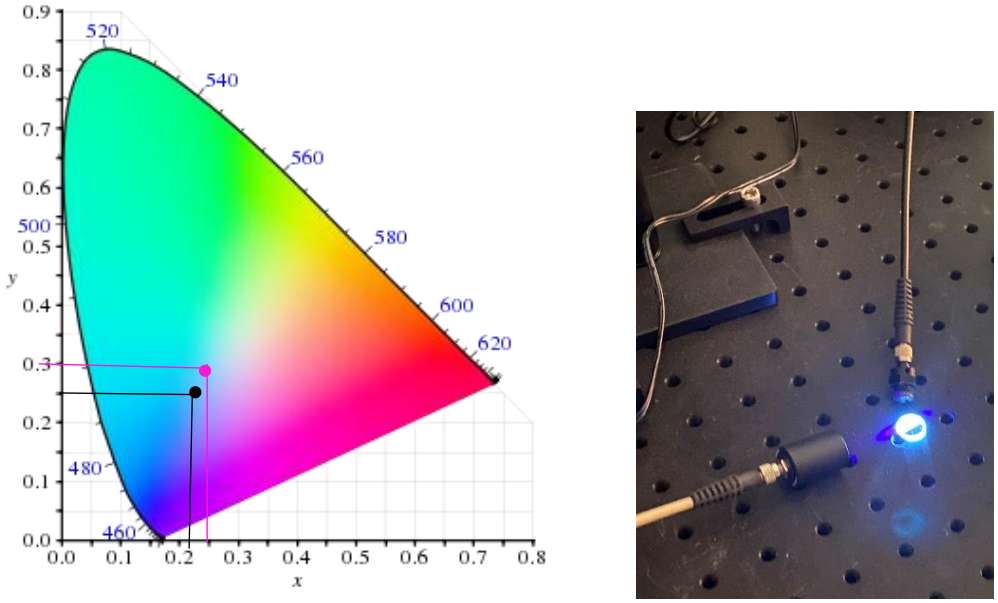

Figure 3.3. a) Chromaticity diagram with x (0.222) and y (0.248) coordinates for T5a_6V (black) and x (0.24) and y (0.30) coordinates for T5C_6V_aged 1min (pink) of PFO (adapted from https://en.wikipedia.org/wiki/CIE_1931_color_space accessed on July,2021, b) Photograph of PFO emission upon excitation at 405 nm

3.1.2. Poly(9,9-dioctylfluorene-*alt*-benzothiadiazole), F8BT

Figure 3.4 shows the result of a F8BT-based LED. It shows a light-onset voltage of ca. 2V, a maximum luminance of 7326 cd/m² reached at 5.5 V and a maximum efficiency of 1.75 cd/A and EQE of 5%. The EL spectrum is shown in Figure 3.5. The emission maximum occurs at 547 nm. F8BT's absorption spectrum shows two peaks at 325 and 475 nm. At variance with the behavior of PFO, these LEDs show a stable EL spectrum. In the calculation of the LEDs luminance a conversion factor of 2526 cd/m²/V was used.

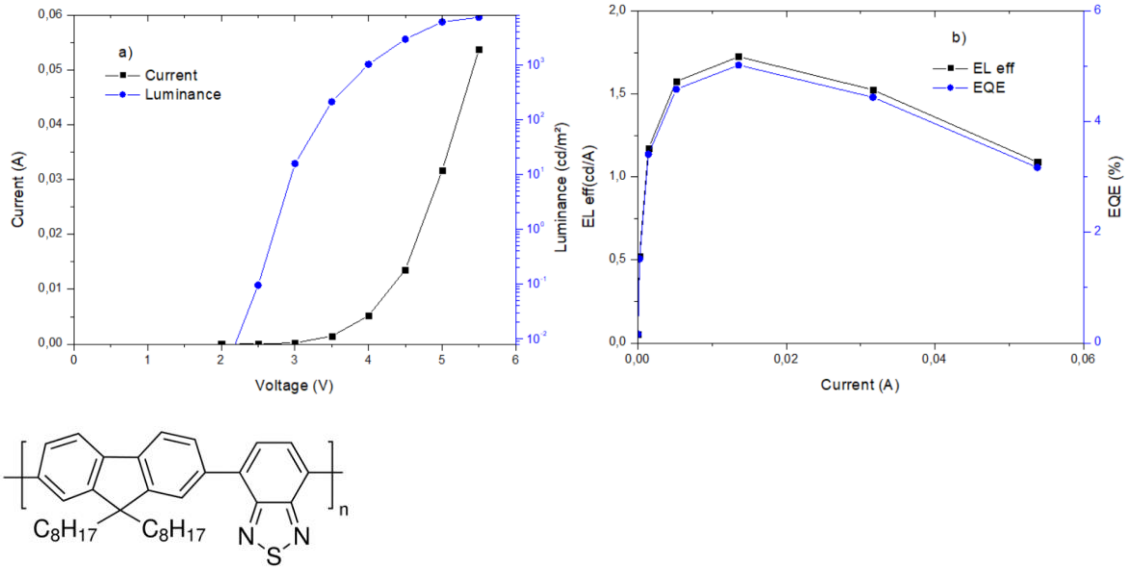

Figure 3.4. a) Current and luminance as a function of the applied voltage of an ITO/PEDOT: PSS/F8BT/Ca/Al LED, b) corresponding electroluminescence efficiency and EQE as a function of the current and c) F8BT´s structure.

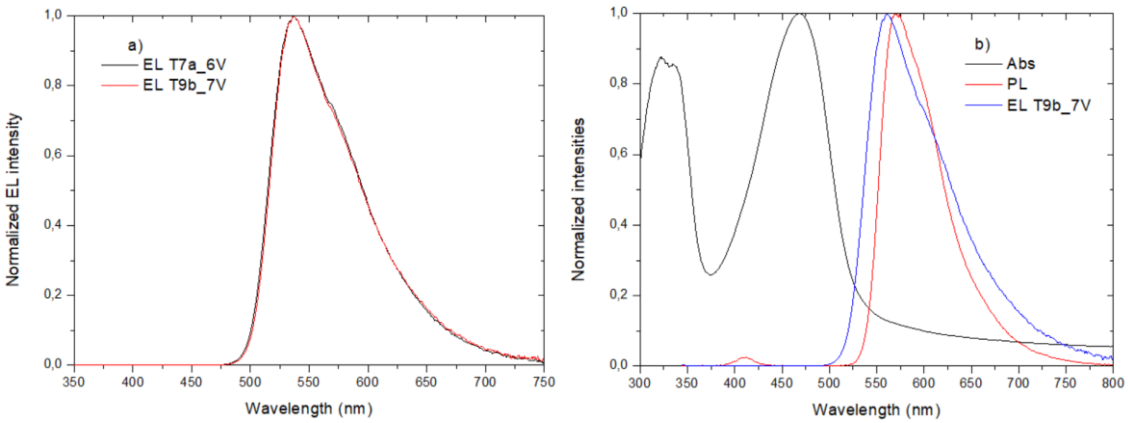

Figure 3.5. a) Normalized EL spectra of F8BT-based LEDs, b) comparison of the EL spectrum with the absorption and photoluminescence (PL) spectra of F8BT films.

3.2. LEDs based on blends

3.2.1. PFO: F8BT (F95)

PFO has been reported to show higher hole than electron mobilities while these mobilities are similar for F8BT (Lee *et al*, 2015); electron mobilities of about 10^{-3} cm^2 /Vs and hole mobilities of about 10^{-2} cm^2 /Vs. As shown in Figure 3.6a, the emission of PFO has a significant spectral overlap with F8BT absorption, thereby fulfilling a condition for efficient energy transfer. In addition, as shown in Figure 3.6 b) the energy level alignment forms a type I heterojunction, which fulfills a second condition for efficient excited state energy transfer. Several studies have shown that blends of these two polymers have led to LEDs with better performance, as compared to LEDs based on neat F8BT (Chen *et al*, 2006). PFO and F8BT have similar HOMO energies, though the LUMO energy of F8BT is lower than that of PFO (Bernardo et al, 2010); for PFO we have LUMO at an energy of -2.1 eV and HOMO at -5.8 eV and for F8BT we have LUMO at -2.4 eV and HOMO at -5.9 eV. Therefore, electron injection from calcium into the LUMO of F8BT is easier than the electron injection in PFO, while hole injection from PEDOT:PSS has similar barriers for both polymers. A blend that was shown to be quite successful for LEDs applications is F95, which is a mixture of 95% of PFO and 5% of F8BT (by weight). Despite the low F8BT content, the LEDs emit in the green, evidencing the efficient energy transfer that occurs from PFO to F8BT. The fact that electrons may be trapped in the LUMO of F8BT (as this has lower energy than the LUMO of PFO) can also promote the exciton formation within F8BT chains. The color coordinates of F95 emission are shown in the chromaticity diagram (CIE) in Figure 3.9, the calculations were based on EL T12d at 5V which can be seen on Figure 3.8a. A photograph of the emitted color is also shown.

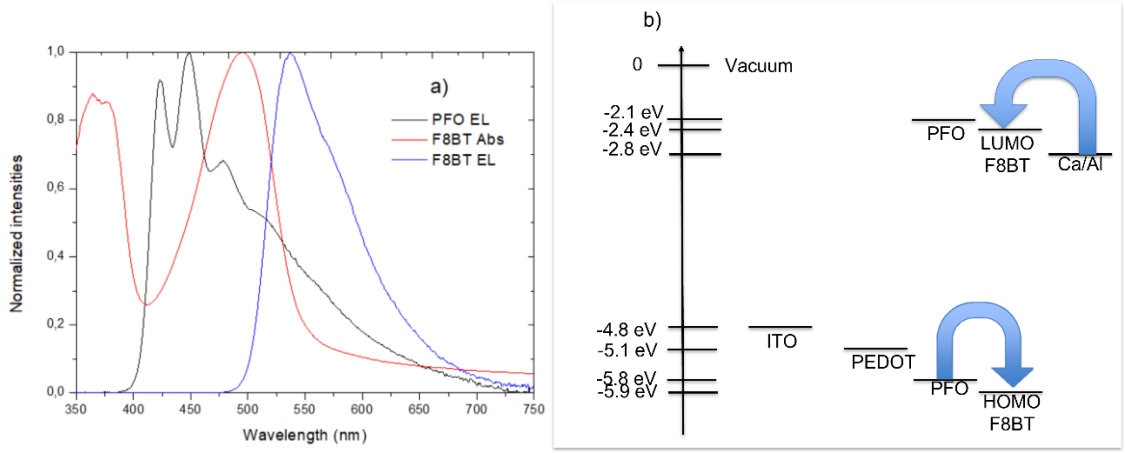

Figure 3.6 a) PFO emission spectrum and F8BT absorption and emission spectra and b) Energy levels diagram for the ITO/PEDOT:PS/F95/Ca/Al LED. The frontier levels energy values are taken from Bernardo *et al* (2010).

Figure 3.7 shows the result of a typical F95-based LED (T12). A light-onset voltage of 2.5 V is observed, reaching a maximum luminance of 18920 cd/m^2 at 7 V. The emission efficiency has a maximum value at 4V (4cd/A and EQE of 1.25%), decreasing upon increase of the flowing current, indicating an increase of the luminescence quenching (a phenomenon known a roll-off). In the calculation of the LEDs luminance a conversion factor of 2765 cd/m^2/V was used.

At the maximum luminance, the efficiency reaches 1.8 cd/A. It is worth noting that, by comparison with the LEDs based on F8BT, a much higher luminance and EL efficiency are obtained, evidencing the benefits of the addition of PFO. It is also remarkable that the presence of only 5% F8BT is enough to obtain an almost pure F8BT emission. This effect is evidenced in Figure 3.8b), where the emission spectra of several LEDs is compared. No significant PFO residual emission is observed. This contrast with the PL spectrum of the F95 blend (Figure 3.8b) where a visible PFO emission remains, though with much lower intensity than that of F8BT. This increased F8BT contribution for EL in comparison with PL indicates that besides energy transfer, the direct exciton formation within F8BT domains provides a significant contribution. Should the excitons be only formed within PFO domains during the OLED driving, we would expect a similar energy transfer efficiency as in PL and, therefore, the EL and PL spectra should exhibit similar PFO contribution.

Figure 3.8c) shows a magnification of the F95 EL spectra of Figure 3.8a) in the PFO emission spectral region. It appears as if the residual PFO emission increases with the driving voltage. This could possibly indicate that higher voltages, with a large number of injected charges, more excitons are formed within PFO domains.

Despite this small effect, the major conclusion is that the efficiency of the combined effects of on-F8BT-sites recombination and the possible exciton transfer from PFO to F8BT are not noticeably affected by the flowing current.

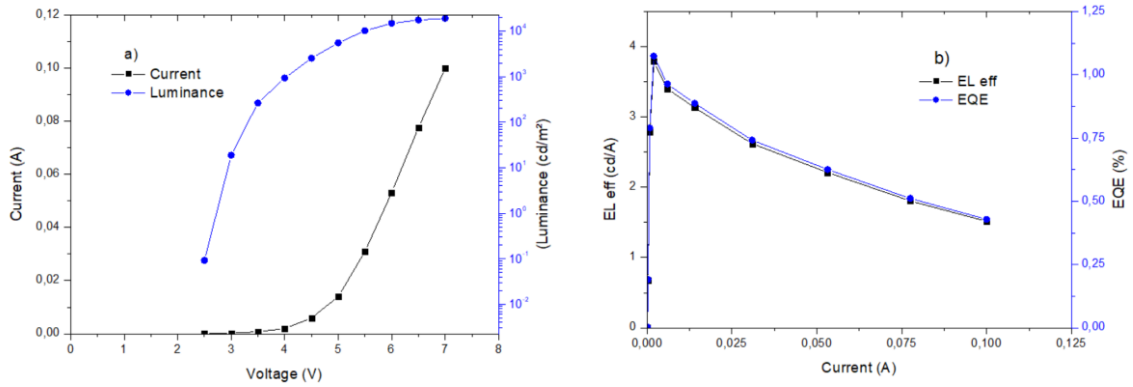

Figure 3.7. a) Current and luminance as a function of the applied voltage of an ITO/PEDOT: PSS/F95/Ca/Al OLED, b) corresponding electroluminescence efficiency and EQE as a function of the current.

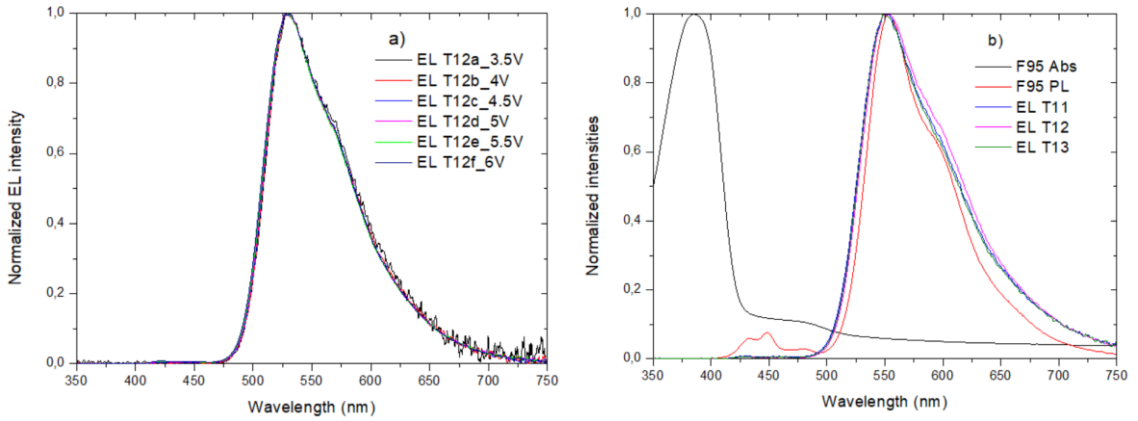

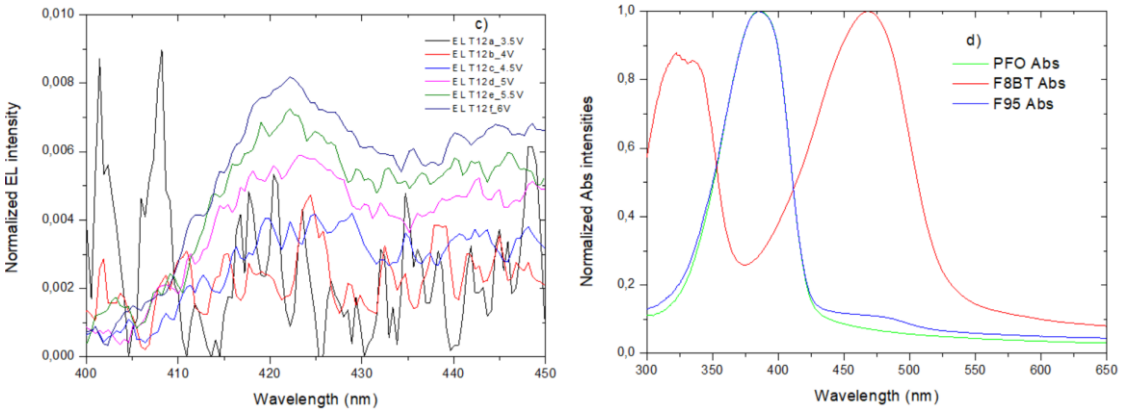

Figure 3.8. a) Normalized EL spectra of F95-based LEDs; b) effect on the EL spectrum and comparison with the absorption and photoluminescence (PL) spectra of F95 films for different LEDs; c) expansion of the area where the PFO emits (400 to 450nm) to assess the relevance of the remnant PFO contribution to the EL spectra and d) comparison between absorption of PFO, F8BT and F95.

Figure 3.8d confirms that using only 5% of F8BT (by weight) the blend absorption spectrum is very similar to that of PFO, as expected. Yet the LED emits is green like F8BT and not blue like PFO.

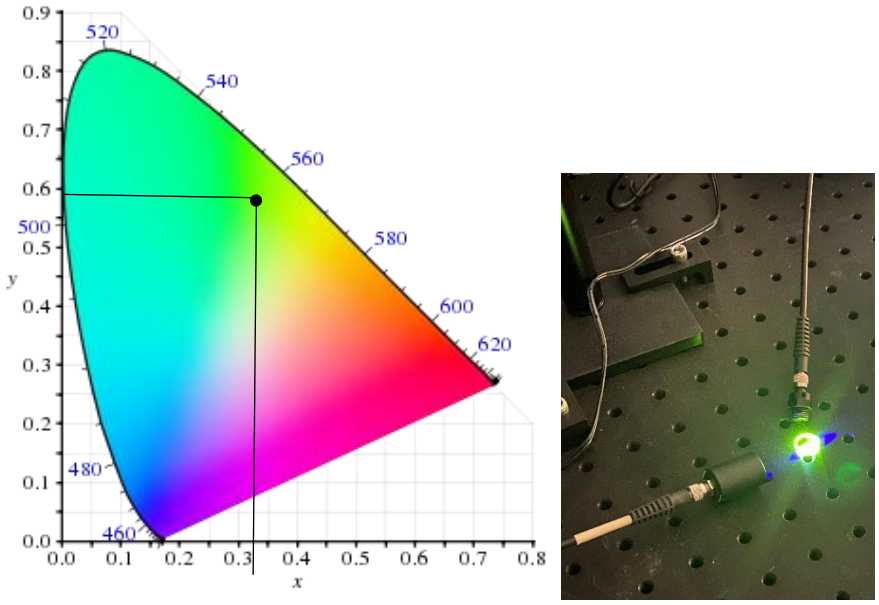

Figure 3.9. a) Chromaticity diagram with x (0.325) and y (0.591) coordinates of the F95 emission (adapted from https://en.wikipedia.org/wiki/CIE_1931_color_space, accessed on July,2021 and b) Photograph of F95 emission upon excitation at 405 nm.

3.2.2. PFO: Ir(dmpq)$_2$(acac) (PFOIr95)

Ir(dmpq)$_2$(acac) is a phosphorescent red emitter. The absorption and PL spectra of the iridium complex were determined in a film made of a small amount of the iridium complex (not weighted) dispersed in polymethylmethacrylate. The absorption shows an onset at 375nm, with a significant spectral overlap with PFO's emission (as shown in Figure 3.10a), fulfilling one of the conditions for excited state energy transfer. The energy level alignment (Figure 3.10b) shows that a second condition, where the energy gap of Ir(dmpq)$_2$(acac) is smaller and this will make it easier for charge carriers. This diagram also shows that the iridium complex can act as efficient charge trapping site, increasing exciton formation and subsequent emission.

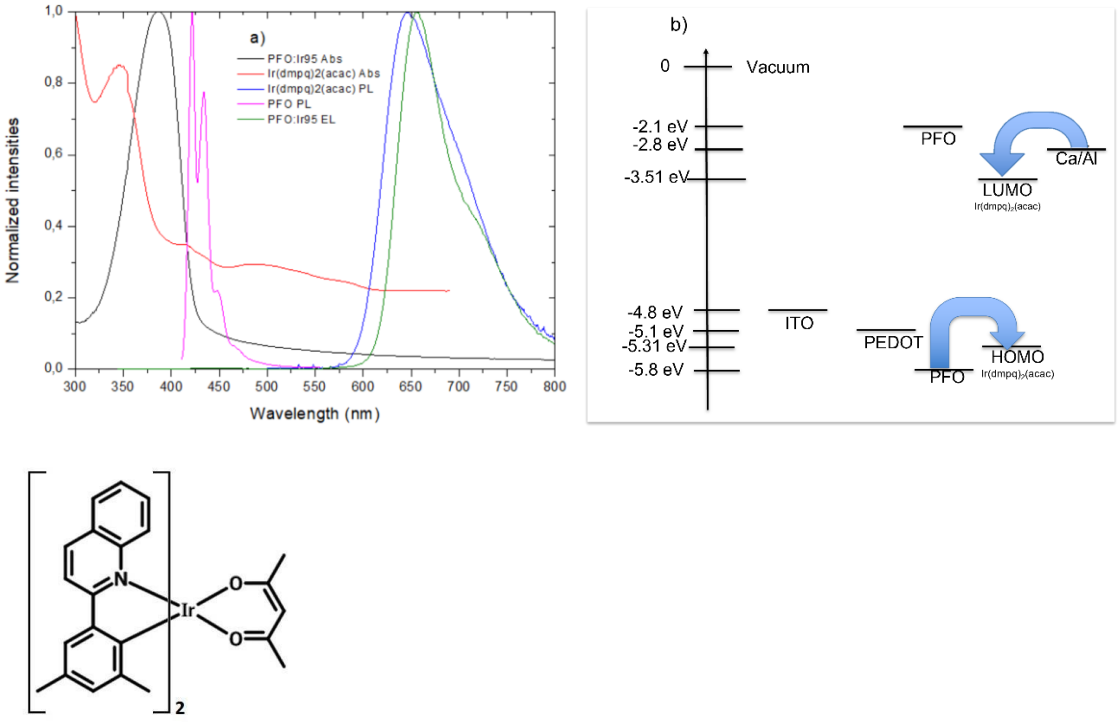

Figure 3.10 a) Absorption and photoluminescence spectra of $Ir(dmpq)_2(acac)$ and the photoluminescence spectrum of PFO compared with blend absorption and emission; b) shows the energy levels diagram for the ITO/PEDOT:PS/PFO:Ir95/Ca/Al LED, the energy values are from Lee *et al* (2013) and Bruno *et al* (2012). c) Molecular structure of $Ir(dmpq)_2(acac)$.

A blend containing PFO and $Ir(dmpq)_2(acac)$, identified as PFOIr95, consisting of 95%, by weight, of PFO, was tested as OLED's active layer. Figure 3.11 shows the performance of a PFOIr95-based LED. A light-onset voltage of 3.5V is observed (in this case we consider the minimum luminance of 10^{-3} cd/m^2), reaching a maximum value of 1580 cd/m^2. The efficiency reaches a maximum value of around 3% at the highest driving voltage. The luminance efficiency in 0.46 cd/A. In the calculation of the LEDs luminance a conversion factor of 925 cd / m2 / V was used.

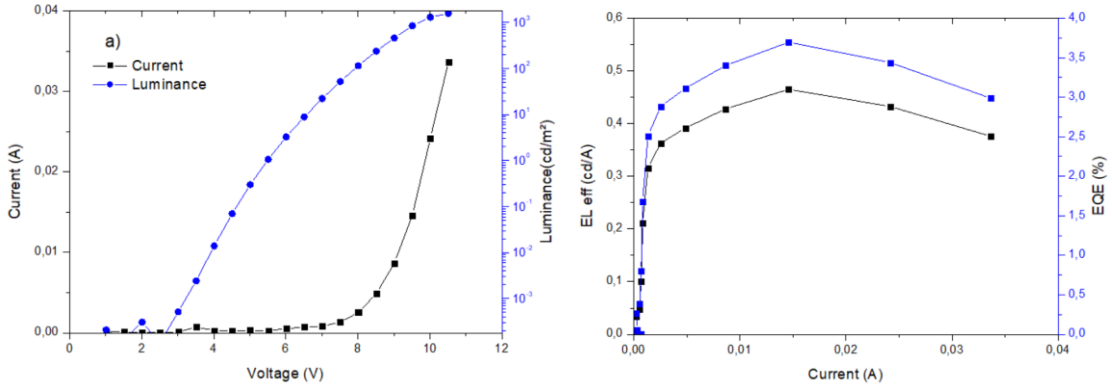

Figure 3.11. a) Current and luminance as a function of the applied voltage of an ITO/PEDOT: PSS/PFOIr95/Ca/Al LED, b) corresponding electroluminescence efficiency and EQE as a function of the current.

The EL spectra, shown in Figure 3.12, of the PFOIr95 OLEDs, are dominated by the iridium complex emission (phosphorescence), without a visible PFO remnant emission.

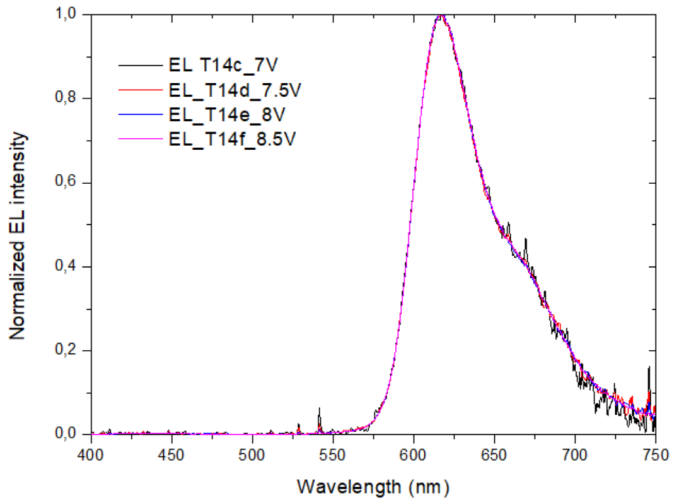

Figure 3.12. Normalized EL spectra of PFOIr95-based.

The color coordinates calculated for the EL spectrum EL T14d_7.5V are shown in the chromaticity diagram (CIE) in Figure 3.13. A photography of the PL emission of the iridium complex obtained upon excitation at 405 nm is also shown in Figure 3.13.

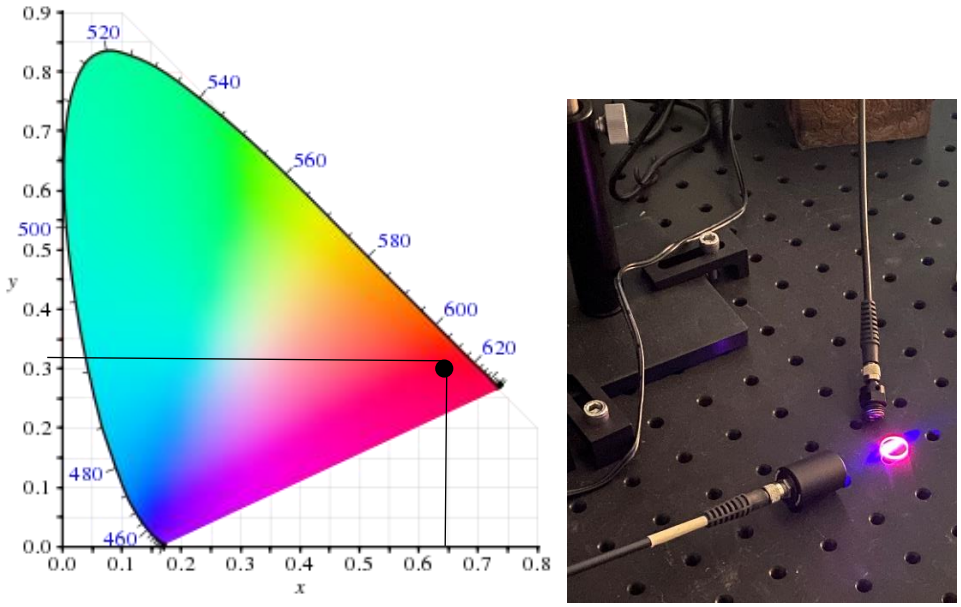

Figure 3.13. a) Chromaticity diagram with x (0.648) and y (0.332) coordinates, based on a picture found in https://en.wikipedia.org/wiki/CIE_1931_color_space at July,2021 and b) Photograph of PFO:Ir95 emission.

The use of the iridium complex, with HOMO and LUMO energies of -5.31 eV and -3.26 eV (Lee *et al*, 2013), which forms with PFO (-5.8 eV and -2.1 eV, respectively, as mentioned above) a type I heterojunction, anticipate that there will be a transfer of the singlet excitons formed within PFO domains to the iridium complex. The singlet excitons transferred to the iridium complex, along with those formed directly at the iridium complex sites, will then undergo an intersystem crossing to the triplet excite state (T_1), from which the red light emission takes place. It also important to mention that the triplet excitons are the majority of the electrically formed excited states within the OLED, those formed at the PFO sites (which would undergo an almost complete non-radiative decay) can be transferred to nearby iridium complex sites (considering that the T_1 state of the iridium complex has lower energy (2.0 eV) (Lee *et al*,2013) than the T_1 of PFO (at 2.3 eV) (Monkman *et al*, 2001). Therefore, the use of the iridium complex should allow an increase of the EQE in comparison with the OLEDS based on neat PFO.

These observations support the observed increase of EQE from ca. 0.12%, for the PFO-based OLEDs (Figure 3.1) to 4.41% obtained for the OLEDS based on PFOIr95.

3.2.3 PVK:Ir(dmpq)$_2$(acac) (PVKIr95)

A blend of poly(N-vinyl carbazole), PVK, and Ir(dmpq)$_2$(acac), containing 95% by weight of PVK, was also studied in LEDs. PVK is known to be a good hole-transporting material and also a violet-blue emitting polymer. In fact, polymer LEDs were first demonstrated by using PVK as emissive layer in 1974's patent by Roger Partridge and later reported in Polymer in 1983 (vol. 24, pages 733, 739, 748 and 755). (Partridge, 2001). This discovery preceded the discovery of LEDs based on conjugated polymers in late 1980's by Richard Friend's group (Burroughes *et al*, 1990), this being the kick-off for the huge development of the polymer-based optoelectronics.

Figure 3.14 shows the performance of an ITO/PEDOT: PSS/PVKIr95/Ca/Al LED. A light-onset voltage of 2.85 V is observed (in this case we consider the minimum luminance of 10^{-3} cd/m^2) reaching a maximum value of 21 cd/m^2. The efficiency reaches a maximum value of 0.007% at the highest driving voltage. The luminance efficiency in 0.0024 cd/A. In the calculation of the LEDs luminance a conversion factor of 253 cd / m2 / V was used.

The efficiency and maximum luminance of this OLED is much smaller than that of the PFOIr95-based OLED. This poor performance is likely due to a poorer electron/hole mobility and lower luminescence efficiency of PVK.

Figure 3.15 shows the absorption of PVK: Ir95 is similar to the neat PVK and have a photoluminescence different from PVK. It is possible to analyze by comparing the EL spectra of PFO: Ir95 and PVK: Ir95 that they are very similar, this reason can be explained by the fact that the Iridium complex is a phosphorescent component, which predominates when the color is emitted.

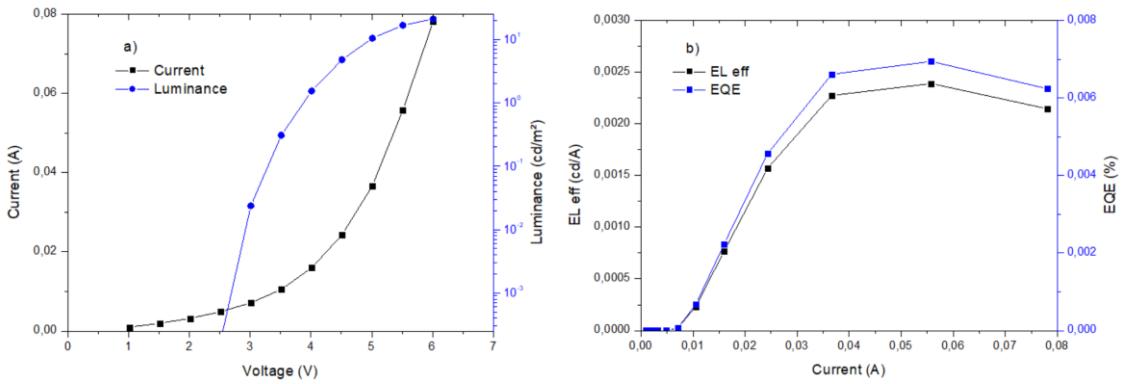

Figure 3.14. a) Current and luminance as a function of the applied voltage, b) corresponding electroluminescence efficiency and EQE as a function of the current.

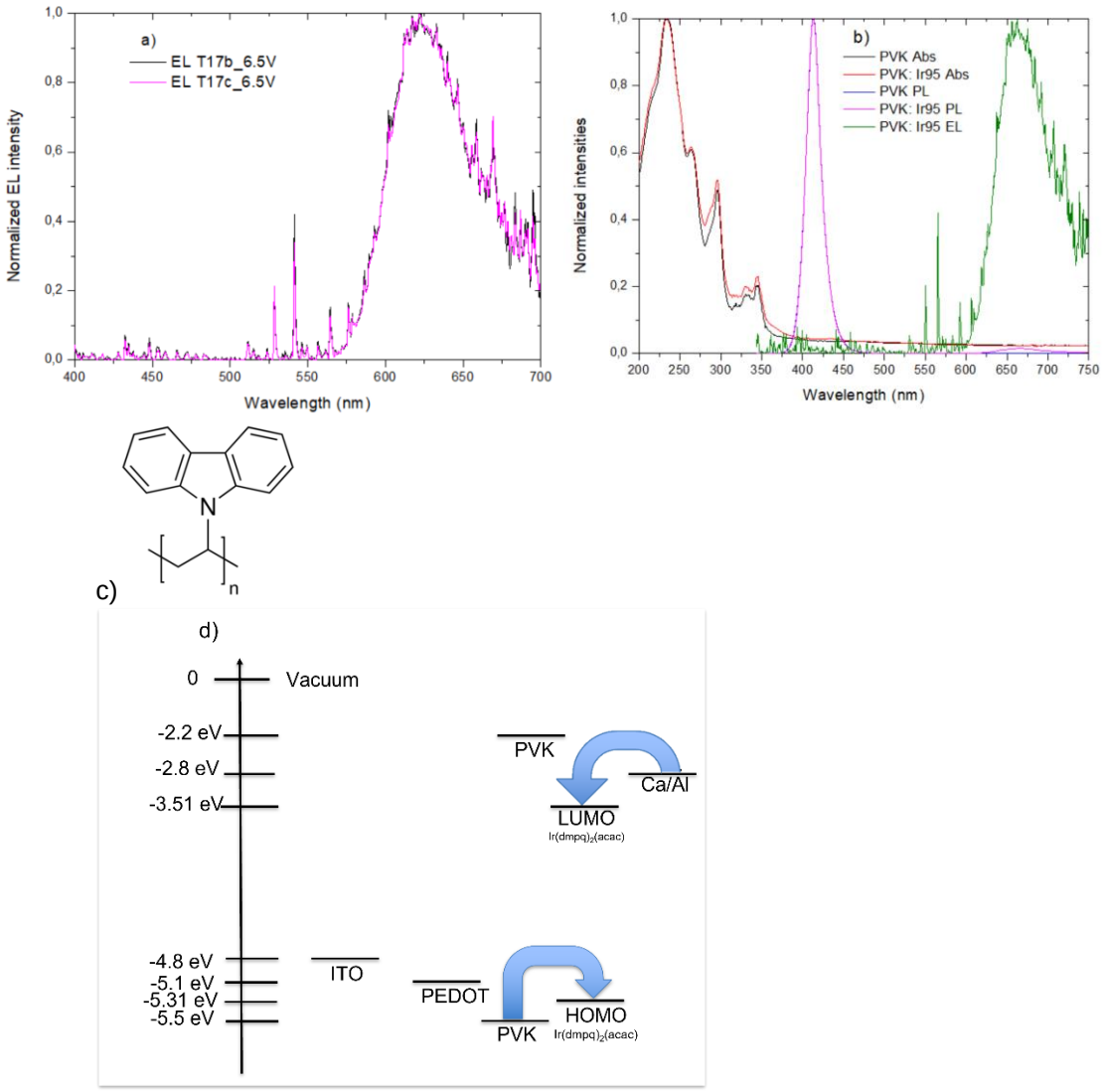

Figure 3.15. a) Normalized EL spectra of PVK:Ir based LEDs; b) effect on the EL spectrum and comparison with the absorption and photoluminescence (PL) spectra of PVK films and PVK: Ir films, c) PVK´s structure and d)) shows the energy levels diagram for the ITO/PEDOT:PS/PVK:Ir95/Ca/Al LED, the energy values are from Lee *et al* (2013) and Bruno *et al* (2012).

3.2.4 PFO: F8BT:Ir

Three different compositions of this ternary system were studied to investigate the influence of that composition of the OLEDs performance. In terms of PFO: F8BT: Ir(dmpq)$_2$(acac) weight ratio, the compositions, with decreasing PFO content, are: 99.82:0.12:0.06; 78:5:17 and 66:4:30.

3.2.4.1 PFO: F8BT: Ir (3)/99.82:0.12:0.06

Figure 3.16 shows the performance of a PFO: F8BT: Ir (3)-based LED. A light-onset voltage of 3 V is observed (in this case we consider the minimum luminance of 10^{-2} cd/m^2), reaching a maximum value of 1468 cd/m^2. The efficiency reaches a maximum value of 0.16% at the highest driving voltage. The luminance efficiency in 0.34 cd/A. In the calculation of the LEDs luminance a conversion factor of 1561 cd / m2 / V was used.

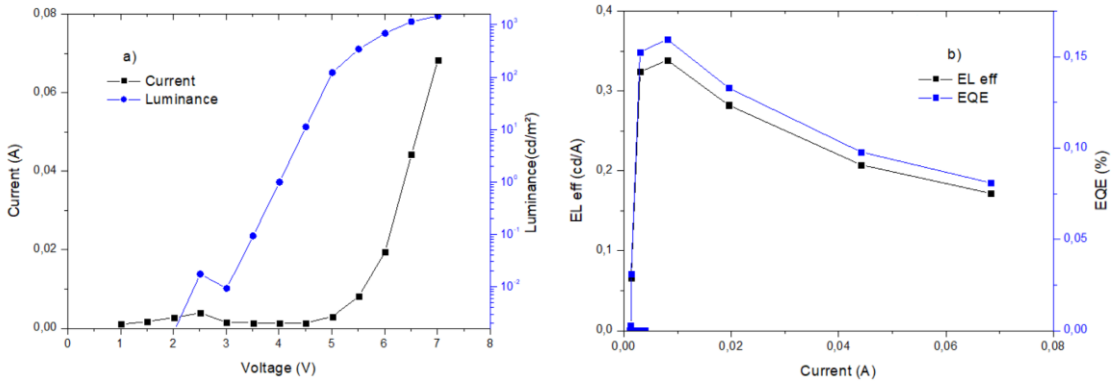

Figure 3.16. a) Current and luminance as a function of the applied voltage, b) corresponding electroluminescence efficiency and EQE as a function of the current.

Figure 3.17 a) shows the EL spectra of two PFO: F8BT: Ir (3)-based LEDs. They show contributions of the three components. In Figure 3.17 b) we compare de absorption spectra of films of neat PFO and PFO: F8BT: Ir (3), confirming the negligible contribution of both F8BT and the iridium complex, as expected in view of their very small content in the mixture.

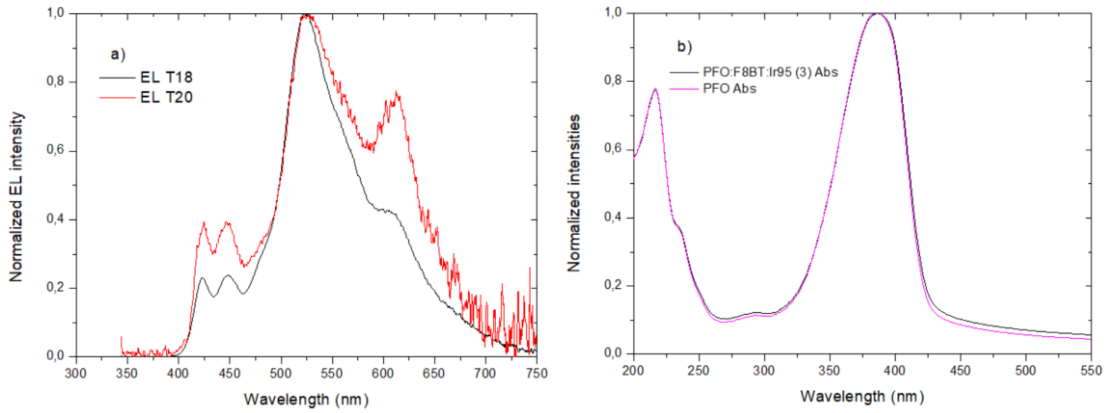

Figure 3.17. a) Normalized EL spectra of PFO: F8BT: Ir(3)based LEDs and b) comparison between the absorption spectrum of films of neat PFO and of PFO: F8BT: Ir (3).

3.2.4.2 PFO: F8BT: Ir (2)/78:5:17

Figure 3.18 shows the performance of a PFO: F8BT: Ir (2)-based LED. A light-onset voltage of 2.5 V is observed (in this case we consider the minimum luminance of 10^{-2} cd/m^2), reaching a maximum value of 1276 cd/m^2. The efficiency reaches a maximum value of 0.12%. The luminance efficiency in 0.138 cd/A. In the calculation of the LEDs luminance a conversion factor of 895 cd / m2 / V was used.

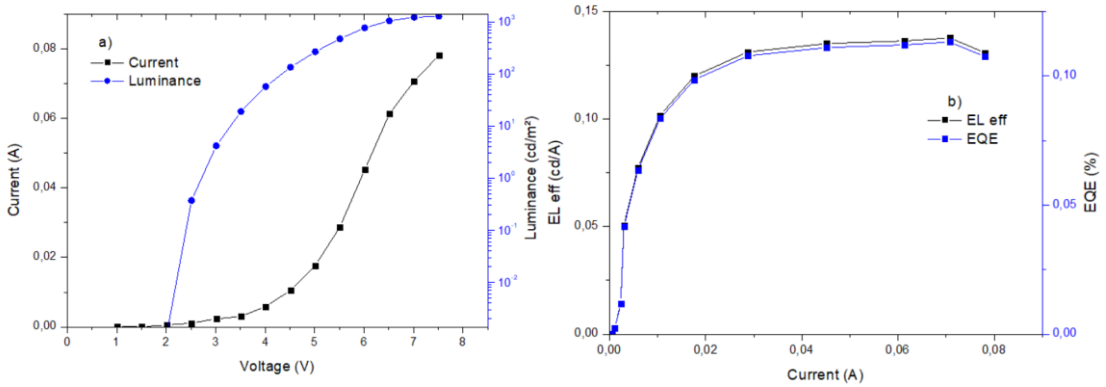

Figure 3.18. a) Current and luminance as a function of the applied voltage for a PFO: F8BT: Ir (2)-based LED and b) corresponding electroluminescence efficiency and EQE as a function of the current.

Figure 3.19 compares the EL spectra of two PFO: F8BT: Ir (2)-based LEDs at various driving voltages.

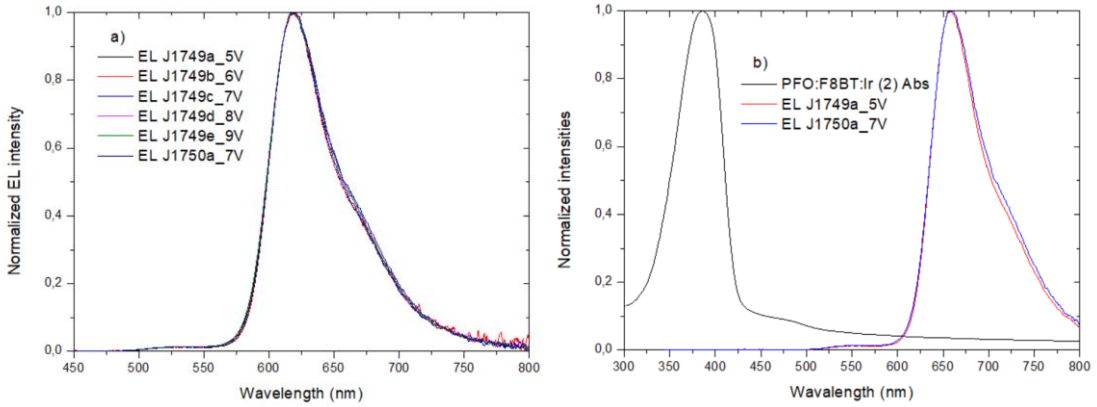

Figure 3.19. a) Normalized EL spectra of PFO:F8BT:Ir (2) based LEDs and b) effect on the EL spectrum and comparison with the absorption spectra of the blend films of different LEDs.

The emission of the OLEDs based on PFO: F8BT: Ir (2) is dominated by the iridium complex phosphorescence, with only a negligible, residual emission of F8BT at around 550 nm. This is the result of the significant increase of the iridium complex content of this blend, when comparing with the emission of the OLEDs based on PFO: F8BT: Ir (3) (Figure 3.17).

3.2.4.3 PFO: F8BT:Ir (1) /66:4:30

A third composition with even higher iridium complex content was prepared, consisting of 64% of PFO; 4% of F8BT and 30% of $Ir(dmpq)_2(acac)$, by weight.

Figure 3.20 shows the performance of a PFO: F8BT: Ir (1)-based LED. A minimum luminance of 10^{-2} cd/m^2 is detected at 2V reaching a maximum value of 1341 cd/m^2. EQE reaches a maximum value of 0.164% corresponding to a maximum luminance efficiency of 0.17 cd/A. In the calculation of the LEDs luminance a conversion factor of 765 cd / m^2 / V was used.

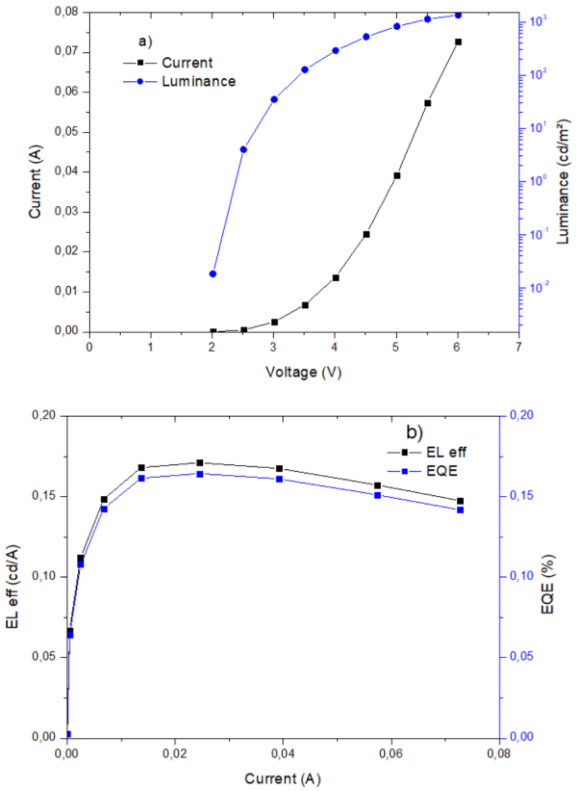

Figure 3.20. a) Current and luminance as a function of the applied voltage of a PFO: F8BT: Ir (1)-based LED, b) corresponding electroluminescence efficiency and EQE as a function of the current.

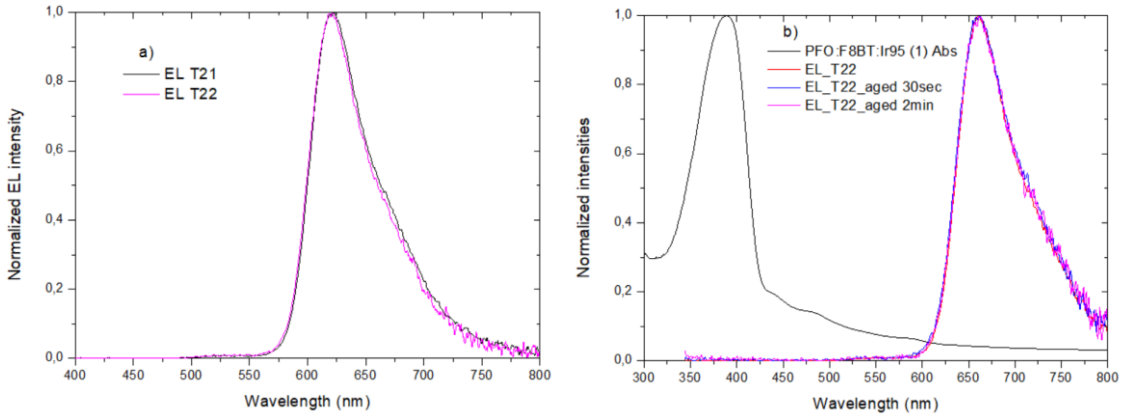

Figure 3.21. a) Normalized EL spectra of PFO:F8BT:Ir (1)-based LEDs and b) aging effect on the EL spectrum and comparison with the absorption spectra of blend films

These results show that OLEDs based on this third composition (64% of PFO, 4% of F8BT and 30% of Ir(dmpq)$_2$(acac)) show a good combination of almost pure red emission with a maximum EQE of 0.16%, when comparing with the other ternary systems with lower iridium complex content. It is also worth pointing out that the residual F8BT emission in these last OLEDs is lower than that observed in the OLEDs based on the PFO: F8BT: Ir (2). The maximum luminance value of the red-emitting OLEDs (based on PFO: F8BT: Ir (2) and PFO: F8BT: Ir(1)) are similar (1276 and 1341 cd/m^2 , respectively). It should be mentioned that, though the red OLEDs based on the binary blend PFOIr95 (Figure3.11) reach a maximum EQE (3%) that is larger than the one obtained for the red OLEDs based on these ternary blends (0.16%), yet its maximum luminance (426cd/m^2) is significantly smaller.

3.2.5 Modification of PEDOT: PSS

It was made a study to change from PEDOT: PSS (AI 4083) to PH1000 because PH1000 has been reported to show higher conductivity and it is important to have a transparent highly conductive polymer that may be used in the fabrication of flexible OLEDs, replacing the ITO.

It was reported that the conductivity of PEDOT: PSS can be increased by addition of dimethyl sulfoxide (DMSO) (Hwang *et al*, 2018). We investigated this process, preparing samples with different DMSO contents (6% and 10%) and measuring the resistance of thin films prepared on glass by spin coating. Table 1.1 compares the resistivity (and conductivity) of the two PEDOT: PSS formulations, as received and after addition of DMSO. It is observed that DMSO promotes an increase of conductivity.

Table 1.1 Electrical properties of various PEDOT: PSS formulations. The distance between contacts is $3x10^{-4}$m. Two different samples were characterised for each component.

Component	Thickness (m)	Width (m)	Section (m^2)	Resistance (Ω)	Resistivity (Ωm)	Conductivity ($Ω\text{-}1.m^{-1}$)
PEDOT: PSS AI 4083	5.0E-08	1.3E-02	6.3E-10	5.1E+06	1.0E+01	9.9E-02
PH1000	6.6E-08	9.7E-03	6.4E-10	1.4E+04	2.7E-02	3.7E+01
PEDOT: PSS AI 4083 + DMSO (10%)	6.0E-08	9.6E-03	5.8E-10	6.3E+06	1.1E+01	8.8E-02
PH1000+DMSO (10%)	7.5E-08	1.2E-02	9.2E-10	4.9E+00	1.4E-05	7.1E+04
PEDOT: PSS AI 4083	5.7E-08	1.2E-02	6.9E-10	4.2E+06	9.1E+00	1.1E-01
PH1000	8.6E-08	1.3E-02	1.1E-09	7.7E+03	2.6E-02	3.8E+01
PEDOT: PSS AI 4083 + DMSO (10%)	6.5E-08	1.3E-02	8.4E-10	7.3E+06	1.9E+01	5.2E-02
PH1000 + DMSO (10%)	1.0E-07	1.2E-02	1.2E-09	4.9E+02	1.9E-03	5.3E+02

3.2.5.1 ITO/PH1000: DMSO/PFO: F8BT: Ir (66:4:30) and Glass/PH1000: DMSO/PFO: F8BT: Ir (66:4:30)

For this ITO/PH1000: DMSO 10%/PFO: F8BT: Ir (66:4:30) we used T31 and T32 devices. T33 and T34 devices refer to Glass/PH1000: DMSO/PFO: F8BT: Ir (66:4:30). Both device types have a concentration of 10% DMSO.

Figure 3.22 shows the performance of a PFO: F8BT: Ir (1) -based LED on ITO/PH1000: DMSO/PFO: F8BT: Ir (66:4:30). A light-onset voltage of 2.1 V is observed (in this case we consider the minimum luminance of 10^{-2} cd/m^2), reaching a maximum value of 724 cd/m^2. The efficiency reaches a maximum value of 0.045% at the highest driving voltage. The luminance efficiency in 0.033 cd/A. In the calculation of the LEDs luminance a conversion factor of 927 cd / m^2 / V was used.

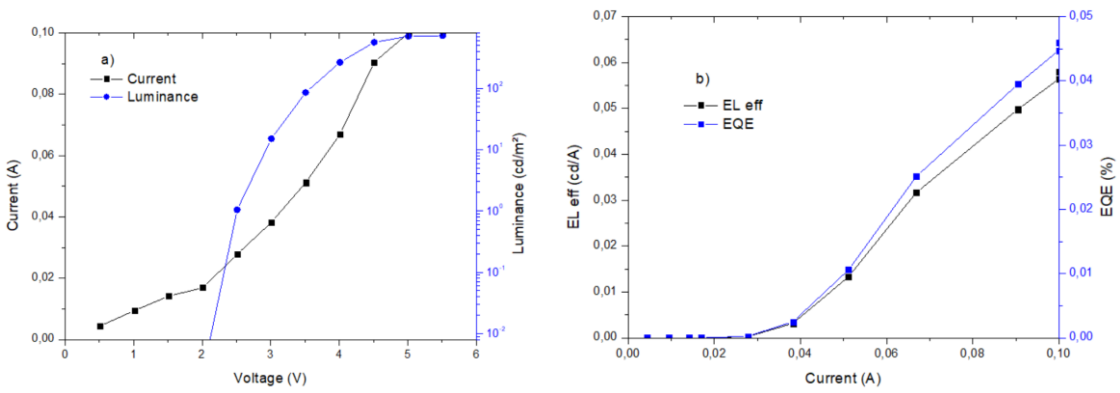

Figure 3.22. a) Current and luminance as a function of the applied voltage for ITO/PH1000: DMSO/PFO: F8BT: Ir (66:4:30)/Ca/Al. b) corresponding electroluminescence efficiency and EQE as a function of the current.

Figure 3.23 shows the performance of a PFO: F8BT: Ir (1)-based LED on Glass/PH1000: DMSO/PFO: F8BT: Ir (66:4:30). A light-onset voltage of 4V is observed (in this case we consider the minimum luminance of 10^{-2} cd/m^2), reaching a maximum value of 212 cd/m^2. The efficiency reaches a maximum value of 0.023% at the highest driving voltage. The luminance efficiency in 0.029 cd/A. In the calculation of the LEDs luminance a conversion factor of 927 cd / m^2 / V was used.

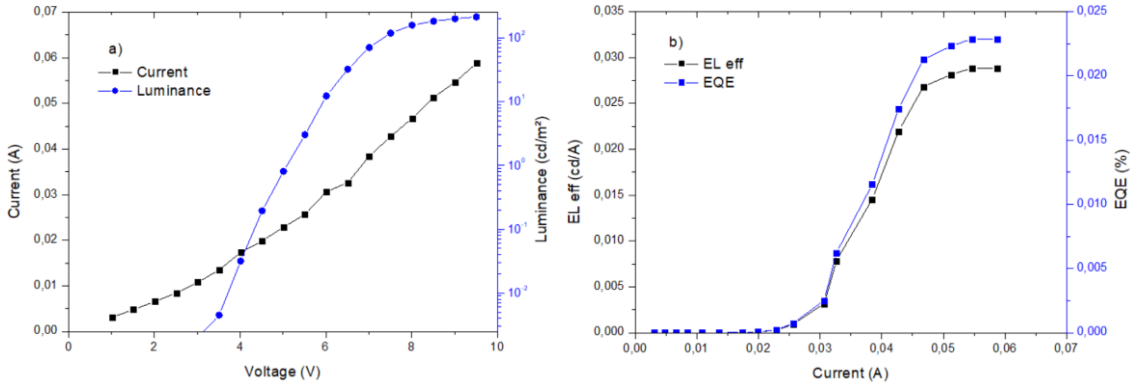

Figure 3.23. a) Current and luminance as a function of the applied voltage for Glass/PH1000: DMSO/PFO: F8BT: Ir (66:4:30)/Ca/Al OLED. b) corresponding electroluminescence efficiency and EQE as a function of the current.

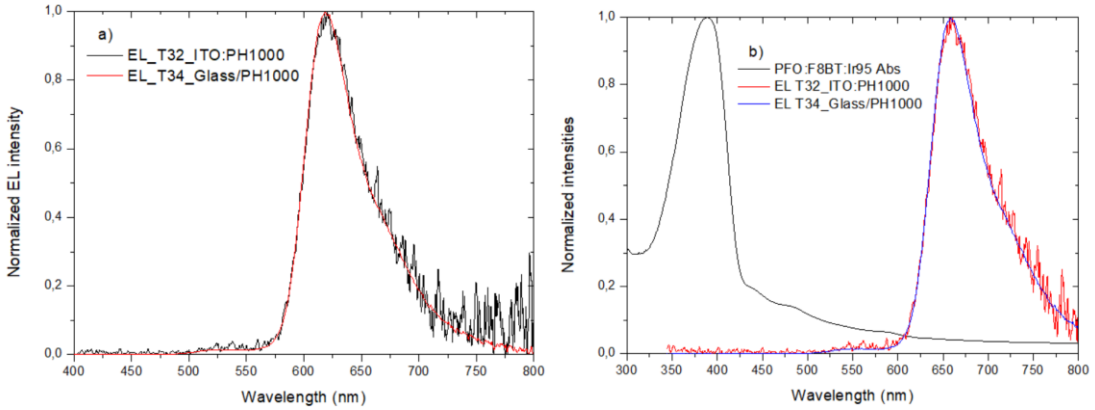

Figure 3.24. a) Normalized EL spectra of PFO_F8BT_Ir-based LEDs and b) effect on the EL spectrum and comparison with the absorption spectra of blend films of different LEDs.

Comparing the two types of LEDs, is possible to verify that the one made on ITO/PH1000: DMSO obtained slightly higher values of luminance, EQE and luminance efficiency when compared with Glass/PH1000: DMSO. To analyse the difference in the luminance and efficiency, the next OLEDs was made using 6% and 10% of DMSO concentration in Glass/PH1000.

3.2.5.2 Glass/PH1000 + 6%DMSO/ PFO: F8BT: Ir (66:4:30) /Ca/Al:

Figure 3.25 shows the performance of this blend LED. A light-onset voltage of 2.85 V is observed (in this case we consider the minimum luminance of 10^{-2} cd/m^2), reaching a maximum value of 234 cd/m^2. The efficiency reaches a maximum value of 0.025% at the highest driving voltage. The luminance efficiency in 0.029 cd/A. In the calculation of the LEDs luminance a conversion factor of 825 cd / m^2 / V was used.

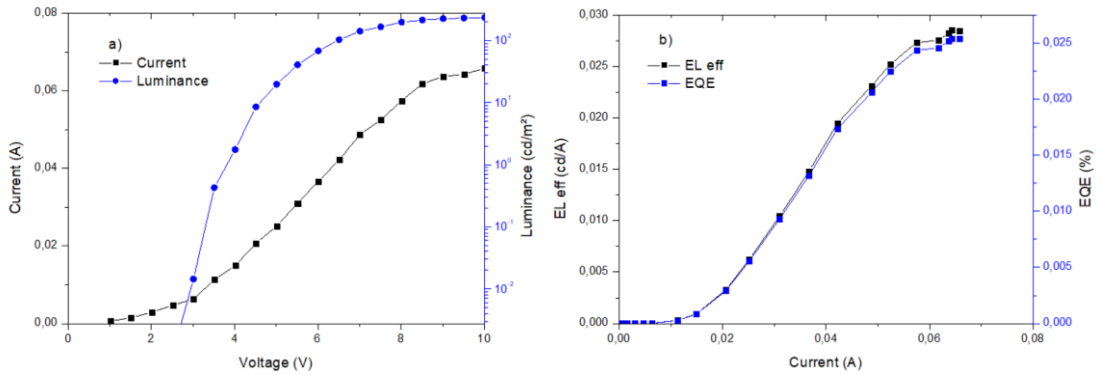

Figure 3.25. a) Current and luminance as a function of the applied voltage for Glass/PH1000 + 6%DMSO/ PFO: F8BT: Ir(1)/Ca/Al. b) corresponding electroluminescence efficiency and EQE as a function of the current.

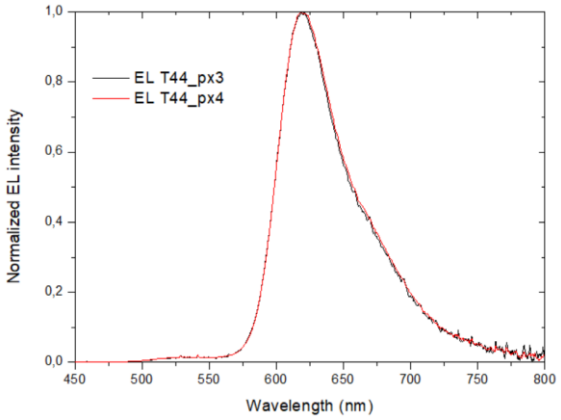

Figure 3.26. Normalized EL spectra for Glass/PH1000 + 6%DMSO/ PFO: F8BT:Ir(1)/Ca/Al LEDs.

Comparing the values obtained in these LEDs and the ones with 10% of DMSO, it is possible to conclude that the luminance, EQE and luminance efficiency improved.

3.2.5.3 Glass/PH1000 + 10%DMSO/PFO: F8BT: Ir (66:4:30) /Ca/Al:

Figure 3.27 shows the performance of this blend LED. A light-onset voltage of 2.5 V is observed (in this case we consider the minimum luminance of 10^{-2} cd/m^2. reaching a maximum value of 314 cd/m^2. The efficiency reaches a maximum value of 0.036% at the highest driving voltage. The luminance efficiency in 0.041 cd/A. In the calculation of the LEDs luminance a conversion factor of 842 cd / m2 / V was used.

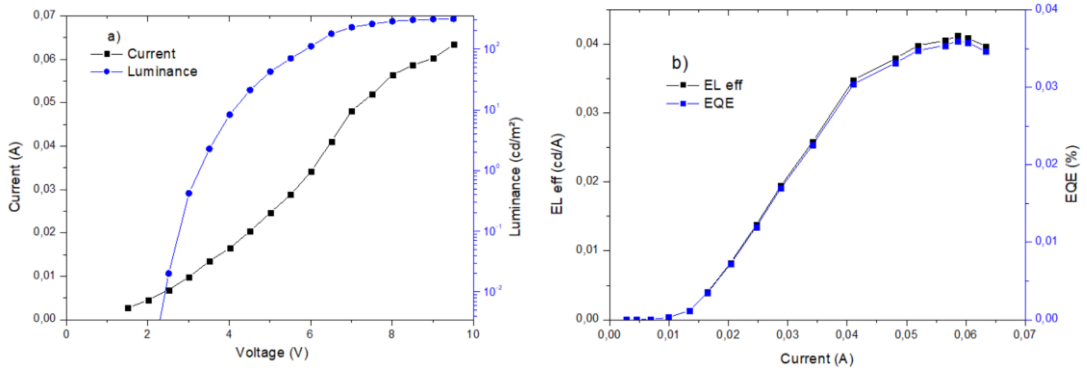

Figure 3.27. a) Current and luminance as a function of the applied voltage for Glass/PH1000 + 10%DMSO/ PFO: F8BT: Ir(1)/Ca/Al.. b) corresponding electroluminescence efficiency and EQE as a function of the current.

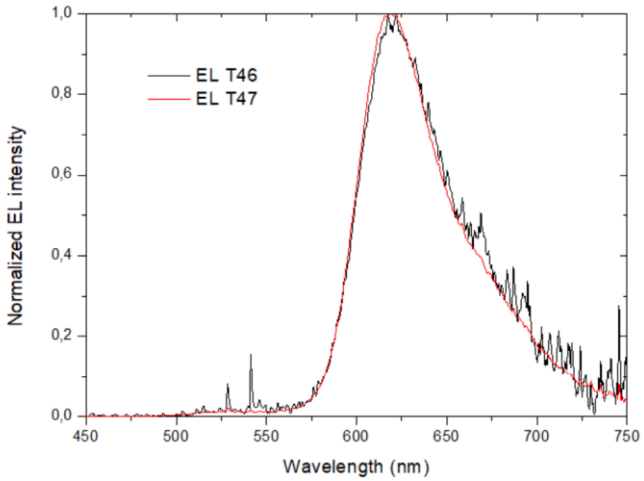

Figure 3.28. Normalized EL spectra of this composition-based LEDs.

Comparing all the LEDs in 3.2.5 it is possible to conclude that LEDs manufactured with ITO/PH1000: DMSO (10%) show higher values for luminance and EQE, but when analyzing the values of LEDs manufactured with Glass/PH1000: DMSO (10%) there is a higher luminance efficiency. One of the reasons that can explain the LED of 3.2.5.1 to have obtained the worst values, could be due to the fact that the mixture of PH1000 and DMSO is not so homogeneous, as the later LEDs were made after the mixture became more homogeneous.

It is concluded that the use of PH1000 with DMSO could be a replacement for ITO.

3.3. Inverted LEDs based on blends and ZnO.

The following devices were prepared:

T50 and 51 - Glass/PH1000+DMSO10%/ZnO/F95/MoO_3/Al

T48 and 49 - Glass/PH1000+DMSO6%/ZnO/F95/MoO_3/Al

T49 was used as representative of the composition of 6% of DMSO and for T51 was used as representative of the composition of 10% of DMSO. Figure 3.29 and Figure 3.30 show the results of this composition-based LEDs.

The use of ZnO offer several improvements in terms of brightness, color, and external quantum efficiency because has potential advantages compared to other wide band gap semiconductors owing to its high exciton binding energy, such relatively high value of exciton binding energy would imply that ZnO has stable and efficient excitonic emission, even above room temperature (Bano *et al*, 2018) which improves and facilitate the production of OLEDs outside of the glove box. Using MoO_3 as electrodes for Inverted LEDs with ZnO is possible to applied negatives voltages.

3.3.1 Glass/PH1000+DMSO6%/ZnO/F95/MoO_3/Al

Figure 3.29 shows the performance of the inverted OLED based on F95 blend. A light-onset voltage of -3 V is observed (in this case we consider the minimum luminance of 10^{-2} cd/m^2), reaching a maximum value of 105 cd/m^2. The efficiency reaches a maximum value of 0.17%. The luminance efficiency in 0.1 cd/A. In the calculation of the LEDs luminance a conversion factor of 447 cd / m^2 / V was used.

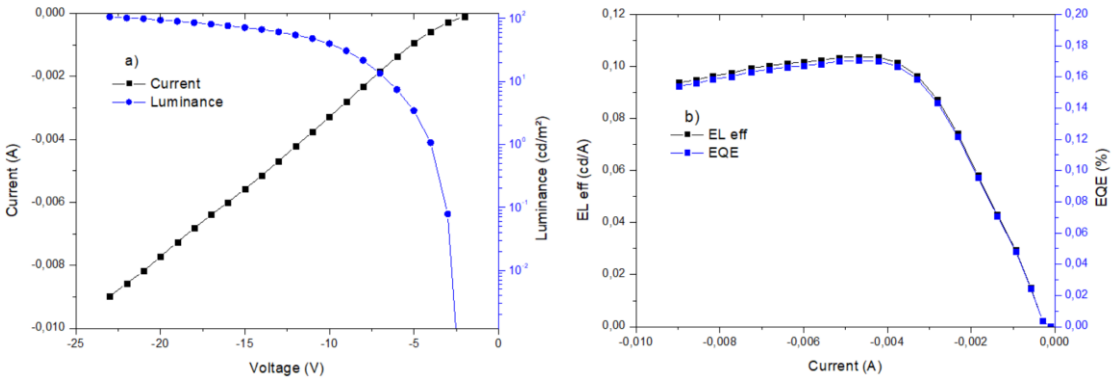

Figure 3.29. a) Current and luminance as a function of the applied voltage for Glass/PH1000+DMSO6%/ZnO/F95/MoO_3/Al. b) corresponding electroluminescence efficiency and EQE as a function of the current.

3.3.2 Glass/PH1000+DMSO10%/ZnO/F95/MoO_3/Al

Figure 3.30 shows the performance of this blend LED. A light-onset voltage of -4.85 V is observed (in this case we consider the minimum luminance of 10^{-2} cd/m^2. reaching a maximum value of 1097 cd/m^2. The efficiency reaches a maximum value of 0.21% at the highest driving voltage. The luminance efficiency in 0.74 cd/A. In the calculation of the LEDs luminance a conversion factor of 2562 cd / m^2 / V was used.

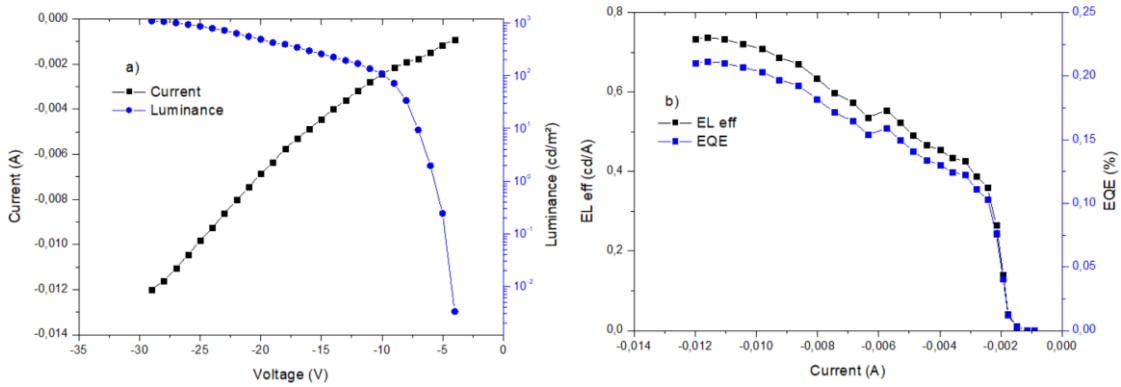

Figure 3.30. a) Current and luminance as a function of the applied voltage for Glass/PH1000+DMSO10%/ZnO/F95/MoO_3/Al. b) corresponding electroluminescence efficiency and EQE as a function of the current.

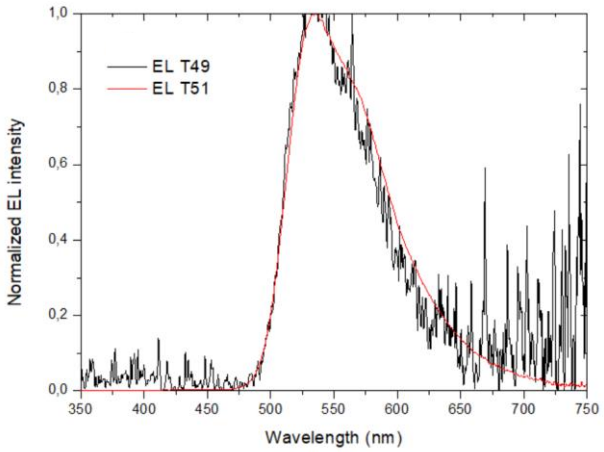

Figure 3.31. Normalized EL spectra of this composition-based LEDs

Based on the data presented above, it is possible to conclude that when we use DMSO with a higher concentration, we obtain higher luminance, EQE and luminance efficiency. To better conclude if this increase in concentration is better for the functionality of LEDs, a study was carried out on the resistivity and conductivity of these concentrations. The results can be seen in table 1.2.

Table 1.2. Different values for conductivity analyzing the different concentrations of DMSO. The distance between contacts is $3x10^{-4}$m. Two different samples were characterised for each component.

Component	Thickness (m)	Width (m)	Section (m^2)	Resistance (Ω)	Resistivity (Ω.m)	Conductivity ($Ω^{-1}.m^{-1}$)
PH1000 + DMSO 6%	9.38E-07	1.25E-02	1.17E-09	5.07	1.86E-05	5.38E04
PH1000 + DMSO 6%	9.28E-07	1.22E-02	1.13E-09	5.93	2.10E-05	4.77E04
PH1000 + DMSO 10%	9.48E-07	1.22E-02	1.16E-09	6.25	2.26E-05	4.43E04
PH1000 + DMSO 10%	8.98E-07	1.11E-02	9.97E-10	6.16	1.92E-05	5.21E04

According to Dimitriev *et al* (2009), the mechanism of the increasing film conductivity using DMSO can be explained via favorable conformational changes of the swelling polymer chains, in this case the organic solvent acts as a secondary dopant. The electrical conductivity dramatically increased as increasing the concentration of DMSO for values between 0 to 6% of DMSO by weight, but after (that the values are approximately equal (Deetuam *et al*, 2015), in this research only two compositions were tested, 6% and 10%.

With this analysis and the experiments from both authors it is possible to conclude that the conductivity is basically the same for both concentrations.

3.4 LEDs on flexible material (PET/ITO)

3.4.1 Poly(9,9-dioctylfluorene), PFO

Figure 3.32 shows the performance of a PFO-based LED on PET/ITO/PEDOT: PSS/PFO/Ca/Al

The device shows a light-onset voltage (voltage at which a luminance of 10^{-2} cd/m^2 is detected) of 3.5 V and reaches a maximum luminance of 202 cd/m^2 at 6V. Above this voltage we find a

performance degradation. The efficiency of the device shows a high value at low current (up to ca. 0.18 cd/A and 0.15%) which decreases and stabilizes at about 0.125 cd/A and 0.08% at the highest luminance values.

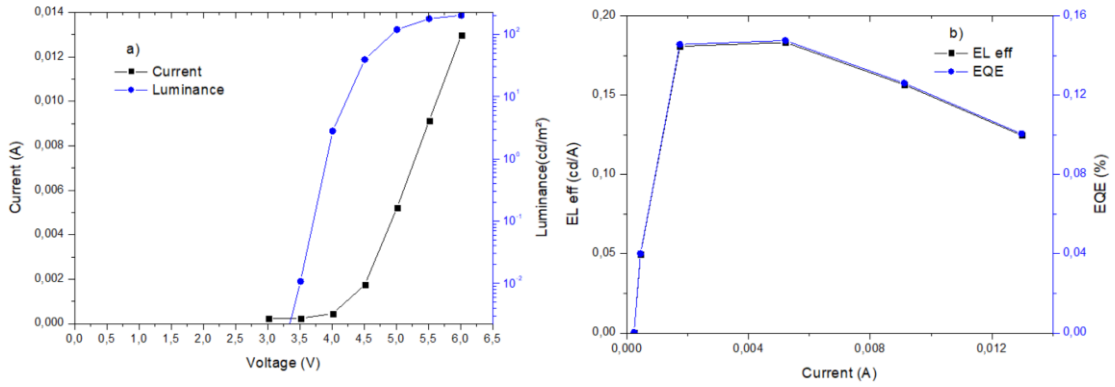

Figure 3.32. a) Current and luminance as a function of the applied voltage for PET/ITO/PEDOT: PSS/PFO/Ca/Al. b) corresponding electroluminescence efficiency and EQE as a function of the current.

3.4.2. Poly(9,9-dioctylfluorene-*alt*-benzothiadiazole)

Figure 3.33 shows the result of a F8BT-based LED. It shows a light-onset voltage is 2.5V. a maximum luminance of 20 cd/m^2 reached at 8 V. The maximum efficiency reached 0.05 cd/A and an EQE of 0.04%. It is surprising the low performance of this device when comparing with the regular F8BT OLED prepared on glass/ITO (Figure 3.4).

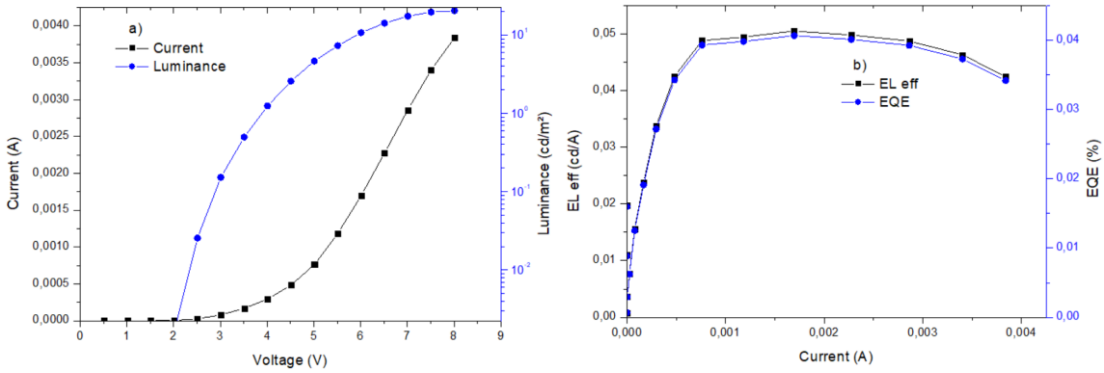

Figure 3.33. a) Current and luminance as a function of the applied voltage for PET/ITO/PEDOT: PSS/F8BT/Ca/Al b) corresponding electroluminescence efficiency and EQE as a function of the current.

3.4.3. PFO: F8BT (F95)

Figure 3.34 shows the result of a typical F95-based LED. A light-onset voltage of 2.5V is observed, reaching a maximum luminance of 663 cd/m^2 at 8 V. The emission efficiency has a maximum value at 0.45 cd/A and EQE of 0.36%.

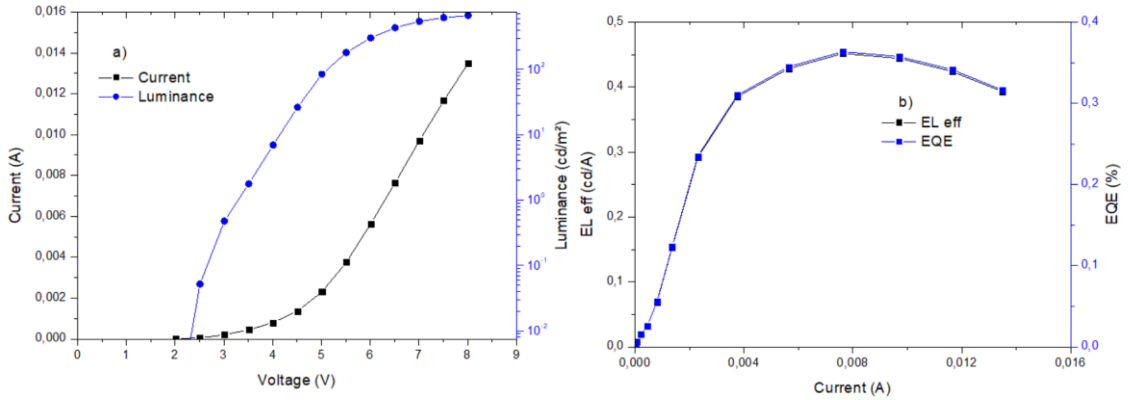

Figure 3.34. a) Current and luminance as a function of the applied voltage for PET/ITO/PEDOT: PSS/F95/Ca/Al . b) corresponding electroluminescence efficiency and EQE as a function of the current.

3.4.4. PFO: F8BT: Ir (1) (66:4:30)

Figure 3.35 shows the performance of a PFO:F8BT:Ir (1) - based LED. A light-onset voltage of 2V is observed (in this case we consider the minimum luminance of 10^{-2} cd/m^2) reaching a maximum value of 154 cd/m^2. The efficiency reaches a maximum value of 0.08% at the highest driving voltage. The luminance efficiency in 0.1 cd/A.

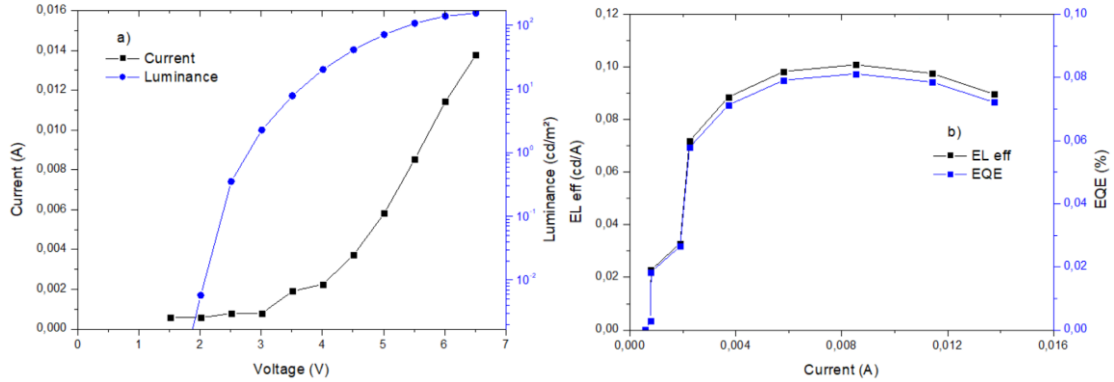

Figure 3.35. a) Current and luminance as a function of the applied voltage for PET/ITO/PEDOT: PSS/PFO: F8BT:Ir95(1)/Ca/Al b) corresponding electroluminescence efficiency and EQE as a function of the current.

To compare the difference between OLEDs produced on PET and OLEDs produced on Glass, a comparison between Luminance, EQE and luminance efficiency is shown in Table 1.3.

Table 1.3. Comparison between different OLEDs produced

Material	Type	Luminance (cd/m^2)	EQE (%)	Luminance efficiency (cd/A)
PFO	PET/ITO	202	0.15	0.18
PFO	GLASS/ITO	348	0.12	0.22
F8BT	PET/ITO	20	0.04	0.05
F8BT	GLASS/ITO	7326	0.5	1.75
F95	PET/ITO	663	0.36	0.45
F95	GLASS/ITO	18920	1.25	4
PFO: F8BT:Ir (66:4:30)	PET/ITO	154	0.08	0.1
PFO: F8BT:Ir (66:4:30)	GLASS/ITO	1341	0.164	0.17

It is possible to conclude that OLEDs produced in flexible materials have lower luminance, EQE and luminance efficiency. When comparing only PFO, it is noticed that the values are very close and compared to F95 these values are very different, this could be explained because F95 is a blend of PFO and F8BTand using only 5% of F8BT the blend is more similar to F8BT than PFO.

When comparing PFO: F8BT: Ir(1) is possible to verify a closely luminance efficiency between them but on flexible material the luminance is 10 times lower.

It is concluded that it is possible to manufacture flexible LEDs with the use of PET/PH1000: DMSO but with lower luminance values and efficiencies than in Glass with ITO.

4 Conclusions

This research was based on the study of the fabrication and characterization of Organic Light Emitting Diodes in ITO-coated glass substrates already found in the literature, for comparison of results for the different compositions;it was also based in the optimization of these same OLEDs for the replacement of ITO as an electrode in order to be possible to manufacture OLEDs without the use of glovebox and the final step were the fabrication and characterization of flexible OLEDs on PET/ITO substrates.

Were prepared and tested OLEDs with different types of polymers (neat and blends). All solutions were prepared and deposited in a glove box filled with nitrogen in order to avoid oxygen and humidity.

For each composition films were prepared various layer thicknesses, methods of deposition, temperature and annealing times. It was necessary the preparation of the differentiated formulation of PEDOT with DMSO to study the conductivity in order to understand which concentration of DMSO would bring better results when applied to OLEDs.

Regarding OLEDs produced on Glass/ITO, a maximum luminance of 18920 cd/m^2 was possible, luminance efficiency of 4 cd/A and EQE of 1.25% for the blend of PFO and F8BT known as F95, while in flexible OLEDs, this same blend achieved 663 cd/m^2 luminance, luminance efficiency of 0.45 cd/A and EQE of 0.36%. The operation of two flexible OLEDs is shown in figures 4.1a and 4.1b.

With this study, it was possible to carry out the fabrication of flexible OLEDs based on PET / ITO, with results related to the literature studied. Its possible to verify on Figure 4.1 examples of the flexibles OLEDs done in this research.

a) 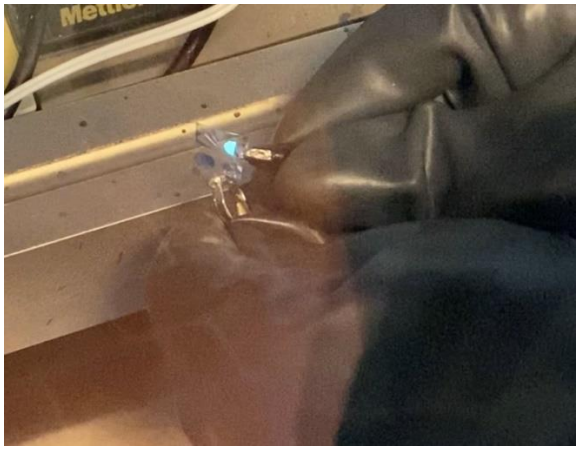

b) 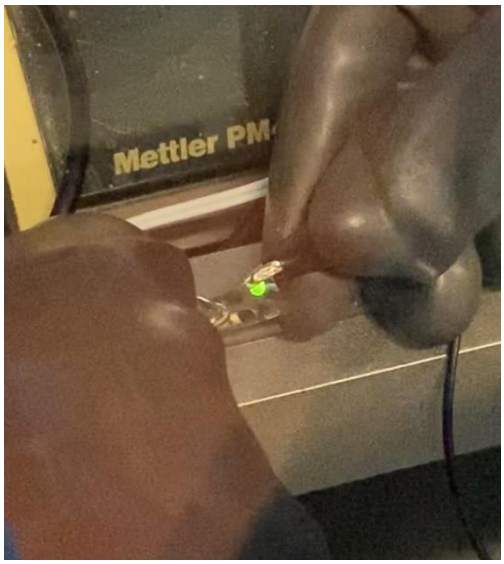

Figure 4.1 Flexible OLED with a) PFO and b) F8BT.

5 Future developments

For future developments, it will be very important to fabricate OLEDs on elastomeric substrates, ideally replacing metallic and oxide-based contacts by polymeric ones to improve the OLEDs stability under cyclic elongation/contraction deformations.

This development can be based on the data obtained in this research, which demonstrates the conductivity of the differentiated formulation of PEDOT with DMSO, in order to avoid ITO and make the OLED completely flexible, and can also be based on the polymers (neat and blends) used here in order to optimize their manufacture and characterization.

The world is always developing, which we didn't even think could exist before, today we don't even imagine how to live without.

References:

Anaya, M., Rand, B., P., Holmes, R., J., Credgington, D., Bolink, H., J., Friend, R., H., Wang, J., Greenham, N., C., and Stranks, S., D., Nat. Photonics. 2019, 13, 818.

Arranz I, Matesanz B, Rosa C de la, et al. The influence of spectral power distribution on contrast sensitivity. Lighting Research & Technology. 2012;44(3):364-376. doi:10.1177/1477153511402890

Bano, N., Hussain, I., Soomro, M.Y., EL-Naggar, A.M. and Albassam, A.A. Solution processable inverted structure ZnO-organic hybrid heterojuction white LEDs. Optical Materials. Volume 79, 2018, Pages 322-326 https://doi.org/10.1016/j.optmat.2018.03.062.

Bernardo, G., Ferreira, Q., Brotas, G., Di Paolo, R.E., Charas, A., Morgado, J. Journal of Applied Physics. 2010.108, 014503 https://doi.org/10.1063/1.3456997

Bruno, A., De Girolamo Del Mauro, A., Mauro, D., Maria, G., Maglione, G., Minarini, C., Nenna, G. and Maglione, M. (2012). Electroluminescence and fluorescence emission of poly(n-vinylcarbazole) and poly(n-vinylcarbazole)-Ir(ppy)3 -based organic light-emitting devices prepared with different solvents. Journal of Photonics for Energy. 25. 10.1117/1.JPE.3.033599.

Buch, J.; Hammond, B. Photobiomodulation of the Visual System and Human Health. Int. J. Mol. Sci. 2020, 21, 8020. https://doi.org/10.3390/ijms21218020

Bull, D.R., Chapter 4 - Digital Picture Formats and Representations, Communicating Pictures, Academic Press, 2014, Pages 99-132, https://doi.org/10.1016/B978-0-12-405906-1.00004-0.

Burroughes, J. H.; Bradley, D. D. C.; Brown, A. R.; Marks, R. N.; MacKay, K.; Friend, R. H.; Burns, P. L.; Holmes, A. B. "Light-emitting diodes based on conjugated polymers". Nature. 347(6293): 539–541 (1990)

Carvalho, C.N., Luis, A., Lavareda, G., Fortunato, E. and Amaral,A. “Effect of thickness on the properties of ITO thin films deposited by RF-PERTE on unheated, flexible, transparent substrates,” Surf. Coatings Technol., vol. 151–152, pp. 252–256, Mar. 2002.

Chandra, H., et al. Open-Source Automated Mapping Four-Point Probe. Materials 2017, 10(2), 110. doi: 10.3390/ma10020110

Chang, Y., Wei, M.-K., Kou, C.-M., Shieh, S.-J., Lee, J.-H., Chen, C.-C., SID Symposium Digest of Technical Papers, 2001, 32: 1040-1043. https://doi.org/10.1889/1.1831736

Charas, A., Morgado, J., Martinho, J.M.G., Fedorov, A., Alcácer, L., Cacialli, F. J. Mater. Chem., 2002,12, 3523-3527

Chen, P., Yang, G., Liu, T., Li, T., Wang, M. and Huang, W. (2006), Optimization of opto-electronic property and device efficiency of polyfluorenes by tuning structure and morphology. Polym. Int., 55: 473-490. https://doi.org/10.1002/pi.1970

Chen, S., Deng, L., Xie, J., Peng, L., Xie, L., Fan, Q. and Huang, W., Adv. Mater., 2019, 22: 5227-5239. https://doi.org/10.1002/adma.201001167

Cohen, E., Lightfoot, E. J. (2011), "Coating Processes", Kirk-Othmer Encyclopedia of Chemical Technology, New York: John
Wiley, doi:10.1002/0471238961.1921182203150805.a01.pub3, ISBN 9780471238966

Deetuam, C., Weise, D., Samthong, C., Praserthdam, P., Baumann, R.
and Somwangthanaroj, A. (2015), Electrical conductivity enhancement of spin-coated PEDOT: PSS thin film via dipping method in low concentration aqueous DMSO. J. Appl. Polym. Sci., 132, 42108, doi: 10.1002/app.42108

de Sá Pereira, D., Przemyslaw D., and Monkman, A. Methods of Analysis of Organic Light Emitting Diodes. Display and Imaging. 2017. 2. 323-337.

Dimitriev, O., Grynko, D., Noskov, Y., Ogurtsov, N., Pud, A. (2009). PEDOT: PSS films—Effect of organic solvent additives and annealing on the film conductivity. Synthetic Metals. 159. 2237-2239. 10.1016/j.synthmet.2009.08.022.

Dodabalapur A. Organic light emitting diodes. Solid State Commun .1997. 102(2–3):259–267

Duan, L., Hou, L., Lee,T., Qiao,J., Zhang, D., Dong, G., Wang, L., Qiu, Y., J. Mater. Chem., 2010,20, 6392-6407 https://doi.org/10.1039/B926348A

Farhan, M.S., Zalnezhad, E., Bushroa, A.R., and Sarhan, A.A.D. “Electrical and optical properties of indium-tin oxide (ITO) films by ion-assisted deposition (IAD) at room temperature,” Int. J. Precis. Eng. Manuf., vol. 14, no. 8, pp. 1465–1469, 2013.

Forrest, S.R., Burrows, P.E., Shen, Z., Gu,G., Bulovic, V., Thompson, M.E., Synthetic Metals, 1997, Volume 91, Issues 1–3, Pages 9-13, https://doi.org/10.1016/S0379-6779(97)03966-0.

Gheidari, A.M., Soleimani, E.A., Mansorhoseini, M., Mohajerzadeh, S., Madani, N. and Kolahi, W.S. “Structural properties of indium tin oxide thin films prepared for application in solar cells,” Mater. Res. Bull., vol. 40, no. 8, pp. 1303–1307, 2005.

Grimsdale, A.C., Chan, K.L., Martin, R.E., Jokisz, P.G., Holmes, A.B., Chemical Reviews, 2009, 109, 987.

Grimsdale, A. C., Jacob, J., Materials Science and Materials Engineering, Elsevier, 2012, 8 Pages 261-282 https://doi.org/10.1016/B978-0-12-803581-8.01483-1.

Grisorio. R.. Suranna. G.P.. Mastrorilli. P.. Nobile. C. Insight into the Role of Oxidation in the Thermally Induced Green Band in Fluorene-Based Systems. Advanced Functional Materials. (2007).17. 538 - 548. 10.1002/adfm.200600083.

Hansen, T., Stokbro, K., Hansen, O., Hassenkam, T., Shiraki, I., Hasegawa, S., Bøggild, P. (2003). Resolution enhancement of scanning four-point-probe measurements on two-dimensional systems. Review of Scientific Instruments - REV SCI INSTR. 74. 10.1063/1.1589161.

Hu, L., Song, J.,Xinxing Y., Zhen, S. and Zaifang, L. (2020). Research Progress on Polymer Solar Cells Based on PEDOT: PSS Electrodes. Polymers. 12. 145. 10.3390/polym12010145.

Hwang, K.H., Kim, D.I., Nam, S., Seo, H., Boo, J.H. (2018). Study on the effect of DMSO on the changes in the conductivity of PEDOT: PSS. Functional Materials Letters. 11. 10.1142/S1793604718500431.

Itskos, G., Xristodoulou, X., Iliopoulos, E., Ladas, S., Kennou, S., Neophytou, M., Choulis, S. (2013). Electronic and interface properties of polyfluorene films on GaN for hybrid optoelectronic applications. Applied Physics Letters. 102. 063303. 10.1063/1.4792211.

Kalyani, N. T.,Swart, H., Dhoble, S.J. Artificial lighting: Origin-impact and future prospectives, in: Principles and Applications of Organic Light Emitting Diodes, Imprint Woodhead Publishing Series in Electronic and Optical Materials, Elsevier, UK, 2017. ISBN 978-0-08-101213-0, pp 87–114 (Chapter 4).

Karzazi, Y., Journal of Materials and Environmental Science 2014. 5. 1-12.

Kido, J., Kimura, M., Nagai, K., Science 1995, 267, Issue 5202, pp. 1332-1334 DOI: 10.1126/science.267.5202.1332

Kijima, Y., Asai, N., Kishii, N., Tamura, Y., IEEE Transactions on Electron Devices,1997, vol. 44, no. 8, pp. 1222-1228, 1997, DOI: 10.1109/16.605458.

Kim, J., Song, M., Seol, J., Hwang H., Park, C. Korean J. Chem. Eng., 22, 643 (2005).

Semiconductors and Energy Level Diagrams. (2021, March 22). Retrieved July 12, 2021, from https://eng.libretexts.org/@go/page/18973

Lee, H., Park, I., Kwak, J., Yoon, D., Kallmann, Y.,Lee, C., (2010). Applied Physics Letters. 96 (15): 153306 DOI:10.1063/1.3400224.

Lee, S., Kim, K.-H., Limbach, D., Park, Y.-S. and Kim, J.-J. (2013), Low Roll-Off and High Efficiency Orange Organic Light Emitting Diodes with Controlled Co-Doping of Green and Red Phosphorescent Dopants in an Exciplex Forming Co-Host. Adv. Funct. Mater., 23: 4105-4110. https://doi.org/10.1002/adfm.201300187

Lee. S. H. Khim. D. Xu. Y. et al. Simultaneous Improvement of Hole and Electron Injection in Organic Field-effect Transistors by Conjugated Polymer-wrapped Carbon Nanotube Interlayers. Sci Rep 5. 10407 (2015). https://doi.org/10.1038/srep10407

Minshall, T., Lane, M., Seldon, S., Probert, D., International Journal of Innovation and Technology Management 2007 04:03, 225-239 https://doi.org/10.1142/S0219877007001107

Misra, A., Kumar, P., Srivastava, R., Dhawan, S.K., Kamalasanan, M.N., Chandra, S. Indian J. Pure Appl. Phys. 2005 .43. 921–925.

Moghe,D., Kabra, D., Chapter 9 - Polymer Light-Emitting Diodes, In Micro and Nano Technologies, Elsevier, 2019, 343-369, https://doi.org/10.1016/B978-0-12-813647-8.00009-6.

Monkman, A.P., Burrows, H.D., Hartwell, L.J., Horsburgh, L.E., Hamblett, I. and Navaratnam, S. Triplet Energies of π-Conjugated Polymers. Phys. Rev. Lett. 86, 1358. 2001. https://doi.org/10.1103/PhysRevLett.86.1358

Morgado, J., Friend, R.H., Cacialli, F. Appl. Phys.Lett. 80 (2002) 2436.

Negi, S., Mittal, P. & Kumar, B. Impact of different layers on performance of OLED. Microsyst Technol 24, 4981–4989 (2018). https://doi.org/10.1007/s00542-018-3918-y

Nuyken, O., Jungermann, S., Wiederhirn, V. et al. Modern Trends in Organic Light-Emitting Devices (OLEDs). Monatsh. Chem. 137, 811–824 (2006). https://doi.org/10.1007/s00706-006-0490-4

Partridge, P. Feedback Friend and Rival. Phys. World 14 (1) 20.2001.

Reichelt K., Jiang, X. “The preparation of thin films by physical vapour deposition methods,” Thin Solid Films, vol. 191, no. 1, pp. 91–126, Oct. 1990.

Reineke, S., Thomschke, M., Lüssem, B., Leo, K., Rev. Mod. Phys. 2013, 85, 1245

Sasabe H., Kido, J., J. Mater. Chem. 2011, 23, 3, 621–630 https://doi.org/10.1021/cm1024052

Sasabe H., Kido J., J. Mater. Chem. 2013, 1, 1699 DOI:10.1039/c2tc00584k

Shafiee, A., Salleh, M., Muhammad, Y. Sains Malaysiana. (2011). 40. 173-176.

Sliney, D., Photochemistry and Photobiology 2007, 83: 425-432. https://doi.org/10.1562/2006-11-14-RA-1081

Smith, T., Guild, J., Transactions of the Optical Society. (1931-32) 33 (3): 73–134. doi:10.1088/1475-4878/33/3/301.

Srivastava, A. M., Ronda, C. R. Phosphors, Electrochem. Soc. Interface 12 (2) (2003) 48–51.

Stewart, M., Howell, R.S., Pires L., Hatalis, M.K., IEEE Transactions on Electron Devices, 2001, vol. 48, no. 5, pp. 845-851, DOI: 10.1109/16.918227.

Sugiyama, K.,Ishii, H., Ouchi, Y., and Seki, K. “Dependence of indium–tin–oxide work function on surface cleaning method as studied by ultraviolet and x-ray photoemission spectroscopies,” J. Appl. Phys., vol. 87, no. 1, p. 295, 2000.

Sun, N., Jiang, C., Li, Q. et al. Performance of OLED under mechanical strain: a review. J Mater Sci: Mater Electron 31, 20688–20729 (2020). https://doi.org/10.1007/s10854-020-04652-5

Suyko, A., " Electronics News, 2009: 20, Associates Programs Source Plus. Web. 9.

Udhiarto, A., Sister, Y., Rini, S., Asvial, M., Munir, B., “Effect of Hole Transport Layer and Electron Transport Layer on the performance of a single emissive layer Organic Light Emitting Diode,” in 14th International Conference on QiR (Quality in Research), QiR 2015 - In conjunction with 4th Asian Symposium on Material Processing, ASMP 2015 and International Conference in Saving Energy in Refrigeration and Air Conditioning, ICSERA 2015, 2016.

Uygun, A., Turkoglu, O., Sen, S., Ersoy, E., Yavuz, A. G., and Batir, G.G. “The electrical conductivity properties of polythiophene/TiO2 nanocomposites prepared in the presence of surfactants,” Curr. Appl. Phys., vol. 9, no. 4, pp. 866–871, 2009.

Wei, Q., Fei, N., Islam, A., Lei, T., Hong, L., Peng, R., Fan, X., Chen, L., Gao, P., Ge, Z., Advanced Optical Materials 2018, 6, 1800512. https://doi.org/10.1002/adom.201800512

Wright, W., D. Transactions of the Optical Society. (1928) 30 (4): 141–164. doi:10.1088/1475-4878/30/4/301.

Appendix:

- **PFO**

For PFO. we used T5 and T6 to analyze. the graphic shows the comparison between them after the normalization of the values.

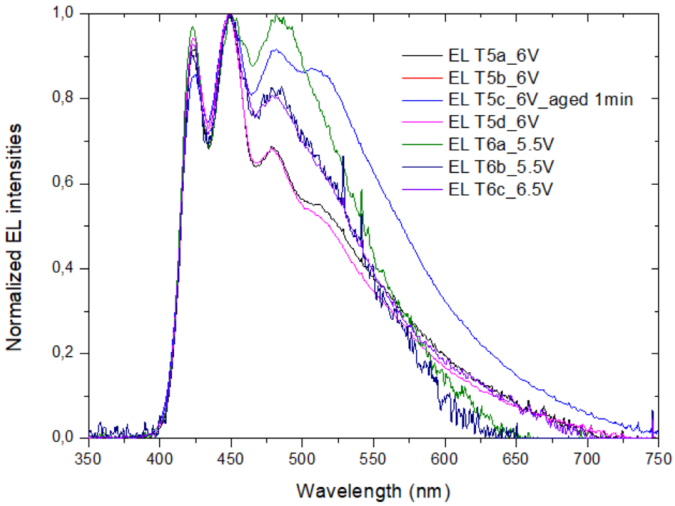

Figure 4.1 Normalized EL spectra of this PFO-based LEDs.

For the calculation. were necessary to calculate first the factor of each one. but it was only used T5a. T5b and T5d which were analyzed in same conditions at 6V.

elT5a: 1360 cd/m^2/V
elT5b: 1349 cd/m^2/V
elT5d: 1338 cd/m^2/V

ElT5b was chosen because it obtains the average result among the others. and the difference between them is low. We can take the elT5b spectrum as representative of PFO LEDs.

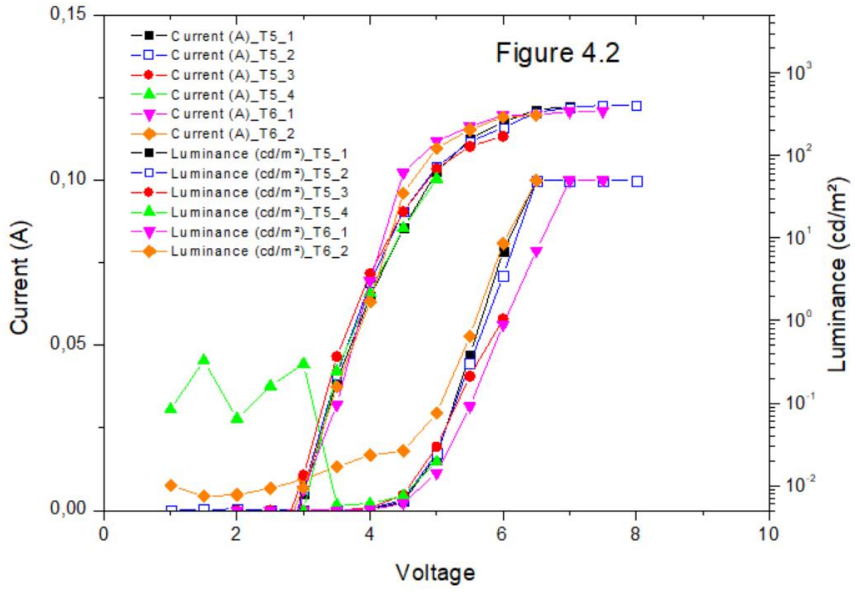

Figure 4.2 Current and luminance as a function of the applied voltage in all pixels for PFO-based LEDs.

With this graphic is possible to conclude that the best option for PFO LEDs is T6 and pixel 1.

- **F8BT**

For F8BT. we used T7 and T9 to analyze. the graphic shows the comparison between them after the normalization of the values. For the calculation. were necessary to calculate first the factor of each one:

elT7a: 2621 cd/m^2/V
elT7b: 2418 cd/m^2/V
elT9a: 2269 cd/m^2/V
elT9b: 2526 cd/m^2/V

ElT9b was chosen because it obtains the average result among the others. and the difference between them is low. We can take the elT9b spectrum as representative of F8BT LEDs which can be seen in the next graphic.

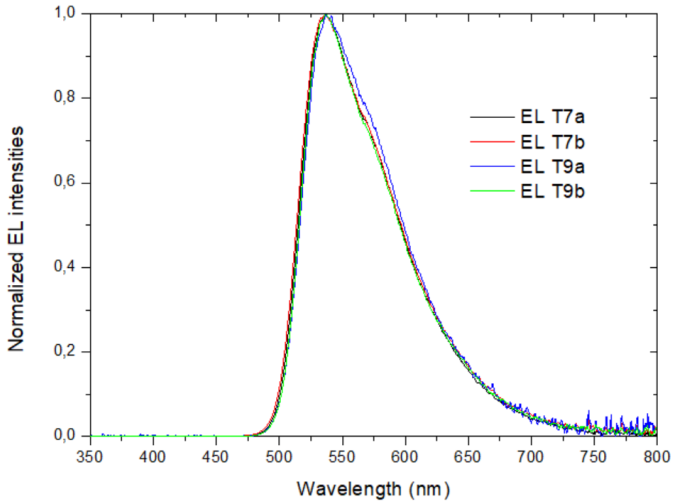

Figure 4.3 Normalized EL spectra of this F8BT-based LEDs.

After that. the calculations using the selected factor were represented on the next graphic for all the LEDs.

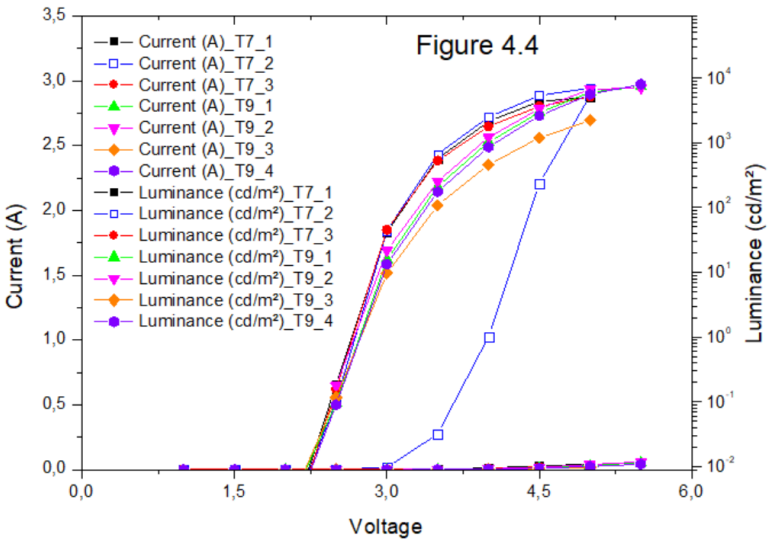

Figure 4.4 Current and luminance as a function of the applied voltage in all pixels for F8BT-based LEDs.

It is possible to conclude that for F8BT the pixel that present better values was pixel 1 for T9.

- **F95**

For F95. we used T11. T12 and T13 to analyze. the graphic shows the comparison between them after the normalization of the values.

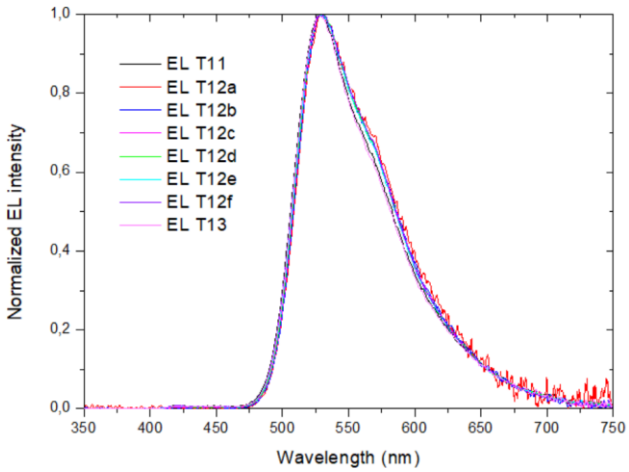

Figure 4.5 Normalized EL spectra of this F95-based LEDs.

For the calculation. were necessary to calculate first the factor of each one in T12 which was analyzed with different values of applied Voltage.

elT12a: 2736 cd/m^2/V
elT12b: 2778 cd/m^2/V
elT12c: 2779 cd/m^2/V
elT12d: 2765 cd/m^2/V
elT12e: 2763 cd/m^2/V
elT12f: 2766 cd/m^2/V

ElT12d was chosen because it obtains the average result among the others. and the difference between them is low. We can take the elT12d spectrum as representative of F95 LEDs.

After that. the calculations using the selected factor were represented on the next graphic:

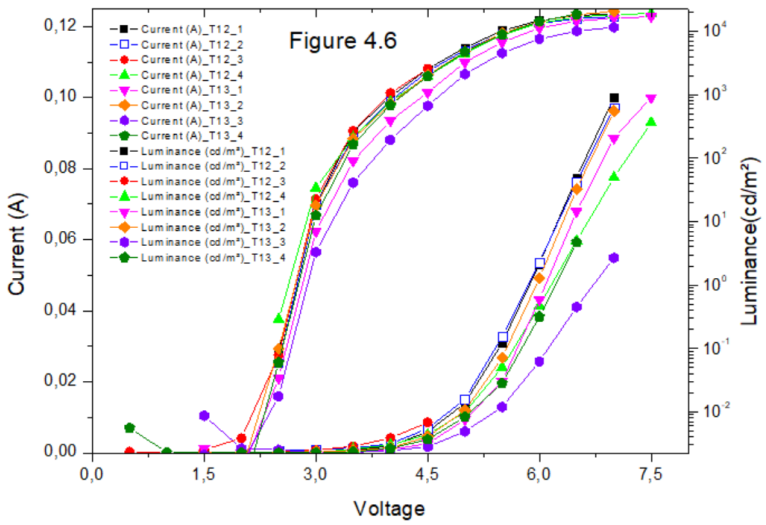

Figure 4.6 Current and luminance as a function of the applied voltage in all pixels for F95-based LEDs.

It is possible to conclude that for F95 the pixel that present better values was pixel 1 for T12.

- **PFO:Ir**

For PFO:Ir only one LED was made T14. The pixel choosen was 3 and was obtained a conversion factor of 895 cd / m2 / V.

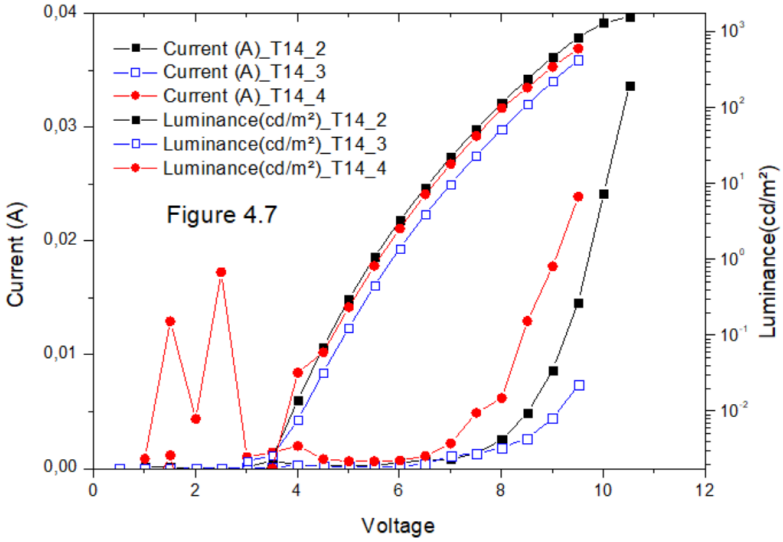

Figure 4.7 Current and luminance as a function of the applied voltage in all pixels for PFO:Ir-based LEDs.

- **PFO: F8BT: Ir(2)**

For PFO F8BT Ir(2). we used J1749 and J1750 to analyze. the graphic shows the results of Luminance calculated by the conversion factor for all pixels.

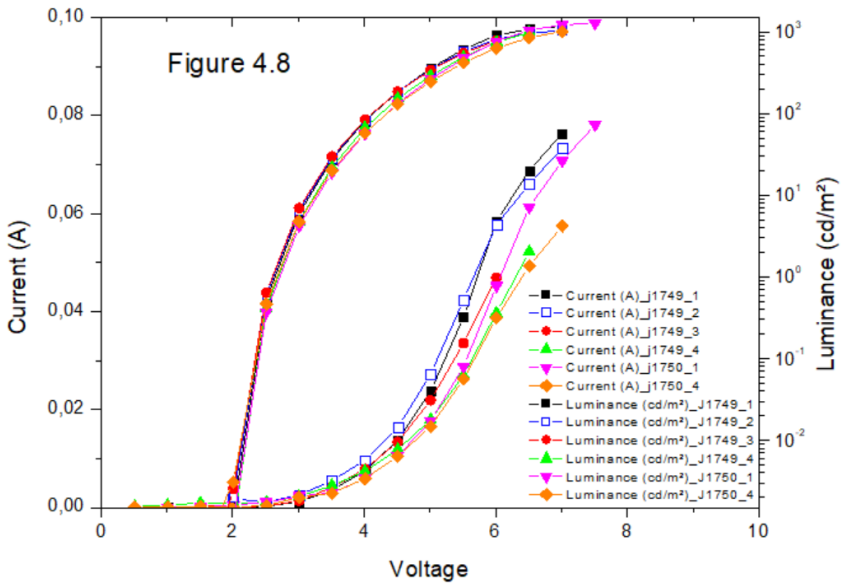

Figure 4.8 Current and luminance as a function of the applied voltage in all pixels for PFO:F8BT:Ir(2) based LEDs.

- **PFO: F8BT: Ir(3)**

For PFO F8BT Ir(3) were made 3 LEDs. T18. T19 and T20. The selected one for the studies was T18. pixel 4. It was obtained a conversion factor of 1560.832 cd/m2/V.

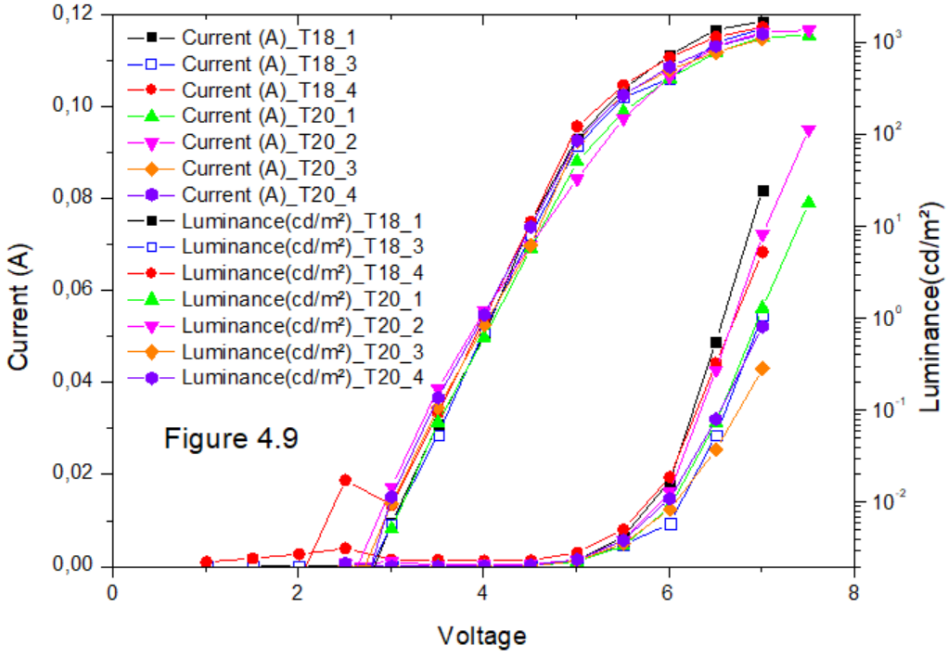

Figure 4.9 Current and luminance as a function of the applied voltage in all pixels. PFO:F8BT:Ir(3) based LEDs

- **PFO: F8BT: Ir(1)**

For PFO F8BT Ir(1) was made 2 LEDs. T21 and T22. The selected one for the studies was T22a which corresponds to pixel 4 with 6V. It was obtained a conversion factor of 765.076 cd/m2/V. The next graphic show the luminance calculated for all LEDs and pixels.

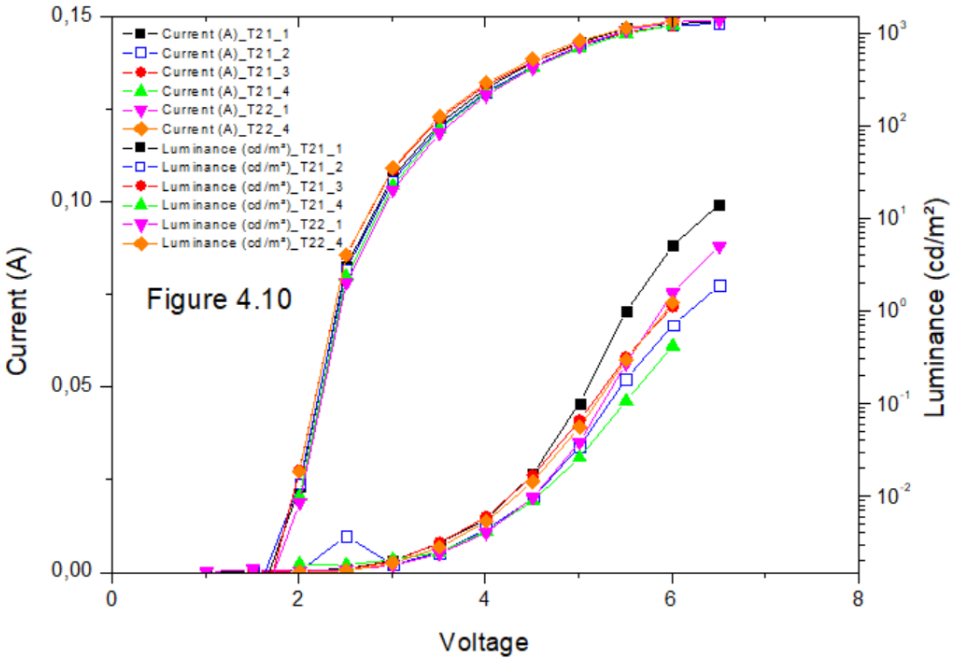

Figure 4.10 Current and luminance as a function of the applied voltage in all pixels PFO:F8BT:Ir(1) based LEDs

- **PFO: F8BT: Ir**

For PFO F8BT Ir was made 3 LEDs. T32. T33 and T34. The selected one for the studies was T32b which corresponds to pixel 1. It was obtained a conversion factor of 927.119 cd/m2/V.The next graphic show the luminance calculated for all LEDs and pixels.

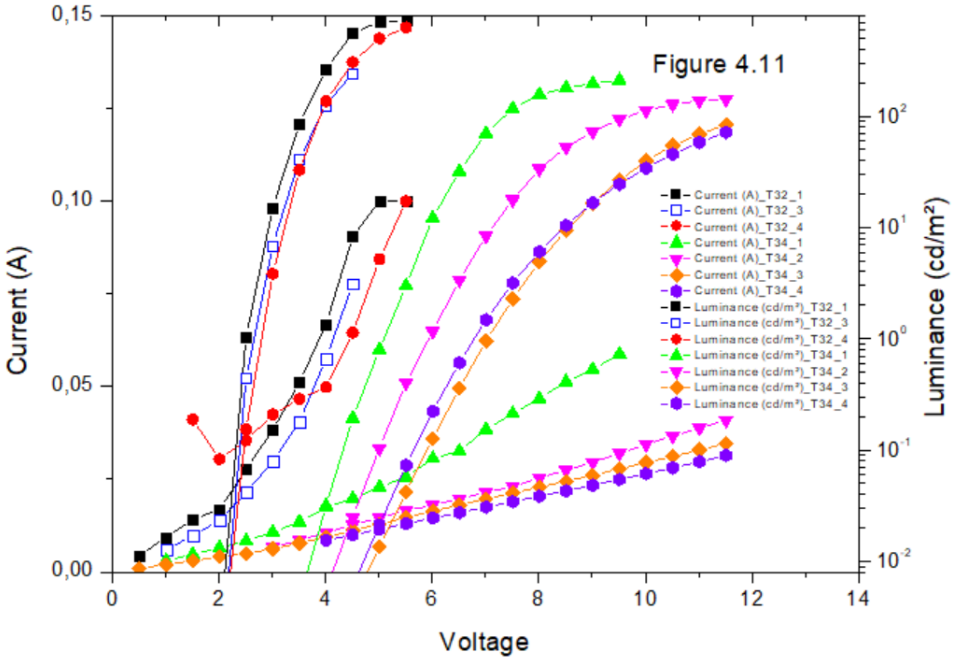

Figure 4.11 Current and luminance as a function of the applied voltage in all pixels. PFO:F8BT:Ir based LEDs

- **PH1000 + 6%DMSO + 66%PFO + 4%F8BT + 30%Ir**

For PH1000 + 6%DMSO + 66%PFO + 4%F8BT + 30%Ir was made 2 LEDs. T44 and T45.The selected one for the studies was T44_3 which corresponds to pixel 3. It was obtained a conversion factor of 824.715 cd/m2/V. The next picture shows the values of luminance for all pixels.

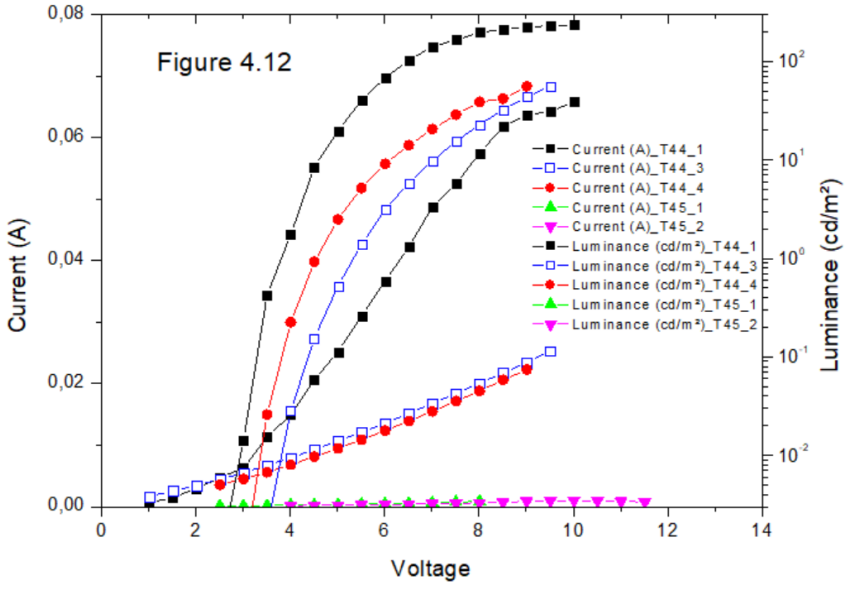

Figure 4.12 Current and luminance as a function of the applied voltage in all pixels for PH1000:DMSO6%:PFO;F8BT:Ir (66:4:30)

- **PH1000 + 10%DMSO + 66%PFO + 4%F8BT + 30%Ir**

For PH1000 + 10%DMSO + 66%PFO + 4%F8BT + 30%Ir was made 2 LEDs. T46 and T47.The selected one for the studies was T46_4 which corresponds to pixel 4. It was obtained a conversion factor of 842.082 cd/m2/V. The next picture shows the values of luminance for all pixels.

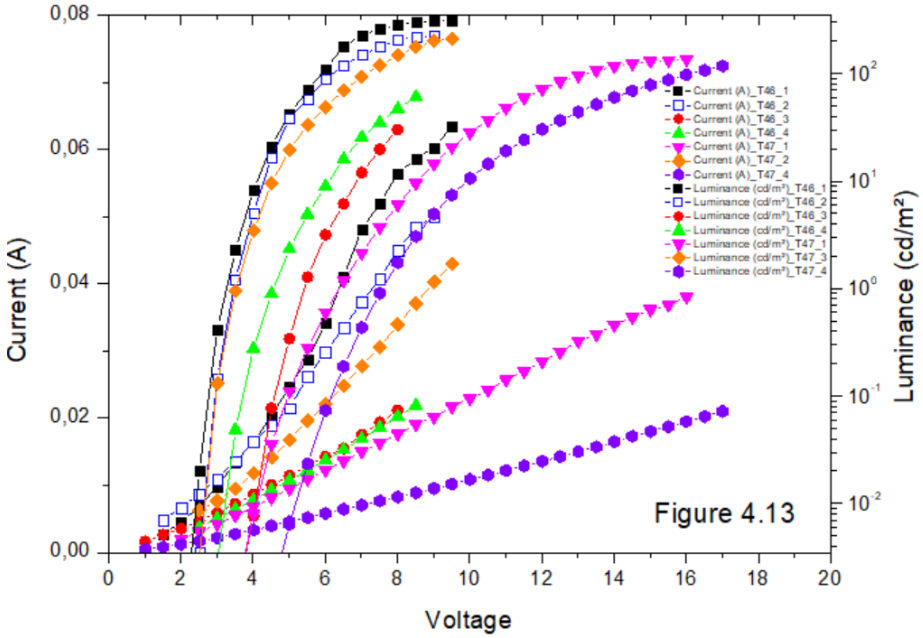

Figure 4.13 Current and luminance as a function of the applied voltage in all pixels for PH1000:DMSO10%/PFO:F8BT:Ir(66:4:30)

- **PFO**

For PFO on flexible material we used only one LED (T52) and in Figure 4.14 shows the comparison between the pixels after the normalization of the values. We can take pixel 1 as representative of PFO.

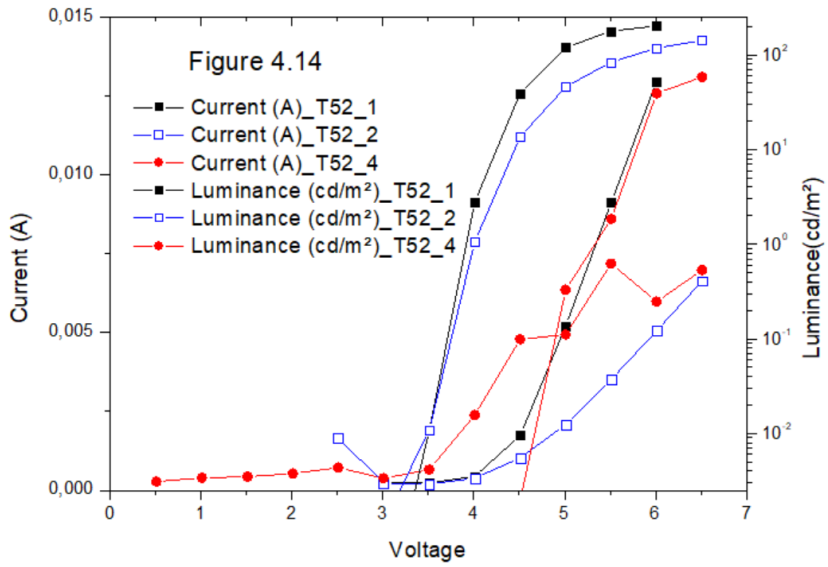

Figure 4.14 Current and luminance as a function of the applied voltage in all pixels for PET:ITO:PFO.

It is possible to verify that during the analysis there is an anomaly on pixel 4. which can be explain by the degradation of the material and the light that emitted was green and not the normal white and there is no contact on pixel 3.

- **F8BT**

For F8BT on flexible material we used only one LED (T53) and in Figure 4.15 shows the comparison between the pixels after the normalization of the values. We can take pixel 4 as representative of F8BT.

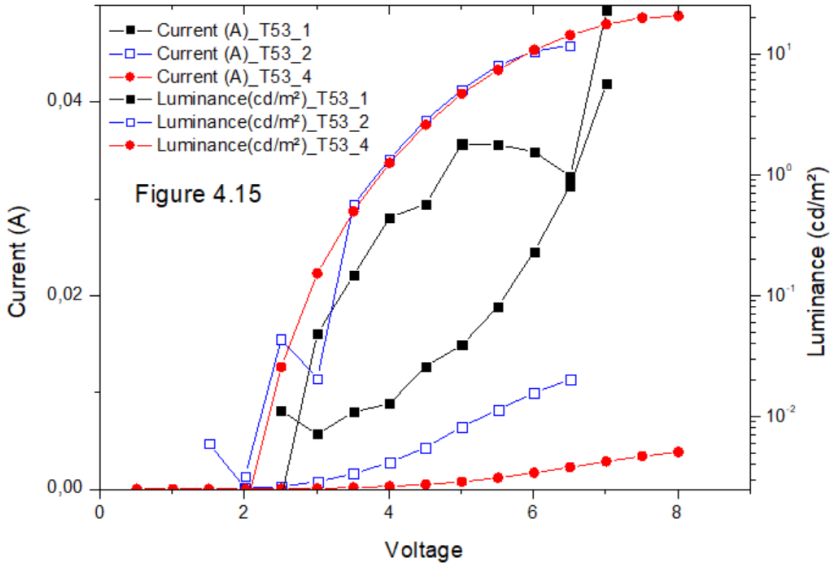

Figure 4.15 Current and luminance as a function of the applied voltage in all pixels for PET:ITO:F8BT.

It is possible to verify that during the analysis there is an irregularity on pixel 1 and there is no contact on pixel 3.

- **F95**

For F95 on flexible material we used only one LED (T54) and in Figure 4.16 shows the comparison between the pixels after the normalization of the values. We can take pixel 4 as representative of F95.

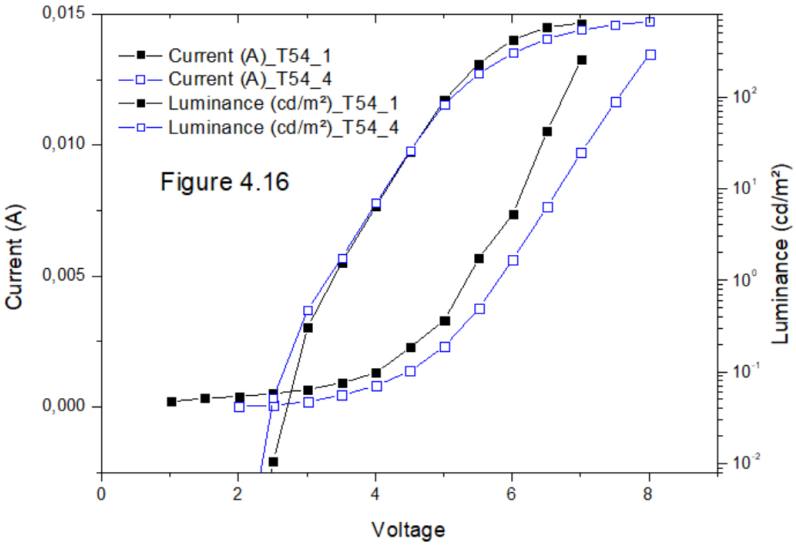

Figure 4.16 Current and luminance as a function of the applied voltage in all pixel for PET:ITO:F95.

It is possible to verify that during the analysis there is no emission on pixel 2 and no contact on pixel 3.

- **PFO: Ir**

For PFO: Ir on flexible material we used only one LED (T55) and in Figure 4.17 shows the comparison between the pixels after the normalization of the values. We can take pixel 4 as representative of PFO: Ir.

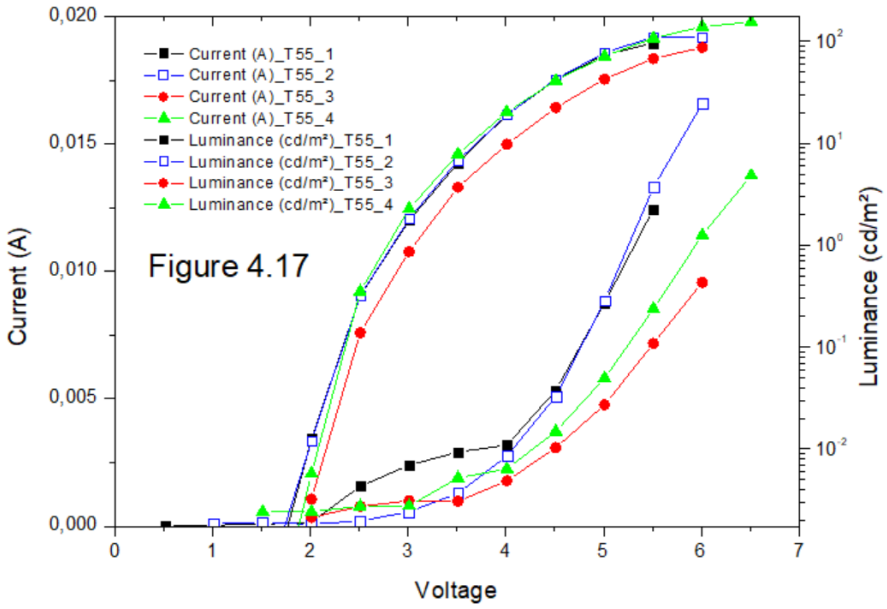

Figure 4.17 Current and luminance as a function of the applied voltage in all pixels for PET:ITO:PFO:Ir.